# Towards green container liner shipping: joint optimization of heterogeneous fleet deployment, speed optimization, and fuel bunkering

Yuzhe Zhao[a], Zhongxiu Peng[a], Jingmiao Zhou[b,*], Theo Notteboom[c,d,e] and Yiji Ma[a]

[a]*Collaborative Innovation Center for Transport Studies, Dalian Maritime University, Dalian 116026, China*
[b]*Business School, Dalian University of Foreign Languages, Dalian 116044, China*
[c]*Maritime Institute, Ghent University, 9000 Ghent, Belgium*
[d]*Faculty of Business and Economics, University of Antwerp, 2000 Antwerp, Belgium*
[e]*Faculty of Sciences, Antwerp Maritime Academy, 2030 Antwerp, Belgium*
*E-mail: zhaoyuzhe@dlmu.edu.cn [Yuzhe Zhao]; pzx2022@dlmu.edu.cn [Zhongxiu Peng]; zhoujingmiao@dlufl.edu.cn [Jingmiao Zhou]; theo.notteboom@ugent.be [Theo Notteboom]; mayiji@dlmu.edu.cn [Yiji Ma]*

Received DD MMMM YYYY; received in revised form DD MMMM YYYY; accepted DD MMMM YYYY

**Abstract**

Container liner shipping companies, under the international shipping carbon reduction indicators proposed by the International Maritime Organization (IMO), must transform two key aspects: technology and operations. This paper defines a green liner shipping problem (GLSP) that integrates the deployment of a heterogeneous fleet, speed determination, and fuel bunkering. The objective is to achieve low-carbon operations in liner shipping, taking into consideration the diversification of power systems, the use of alternative fuels in ships, and the continuous improvement of alternative fuel bunkering systems. For this purpose, we present a bi-objective mixed integer nonlinear programming (BO-MINLP) model and develop two methodologies: an epsilon-constrained approach and a heuristic-based multi-objective genetic algorithm (MOGA). We validate the effectiveness of our model and methods through a case study involving container ships of various sizes deployed on intra-Asian short sea routes by SITC International Holdings Co., Ltd. (SITC). The experimental results highlight the crucial role of dual-fuel (DF) ships in the pursuit of low-carbon strategies by liner companies, with LNG and ammonia dual-fuel ships being the most widely used. Additionally, fuel cell (FC) ships, particularly those powered by ammonia and hydrogen, demonstrate significant carbon reduction potential. Furthermore, ships with larger container capacities have a greater cost advantage. For the GLSP, speed determination is an auxiliary decision, and the lowest speed is not necessarily the optimal choice. Decision-makers must carefully balance competing economic and carbon emission reduction objectives, as deploying more alternative fuel ships may increase fuel bunkering and fuel consumption, resulting in a higher total operating cost.

*Keywords:* liner shipping; heterogeneous fleet deployment; speed determination; fuel bunkering; carbon emission

## 1. Introduction

In 2022, carbon dioxide ($CO_2$) emissions from international shipping constituted approximately 2% of global energy-related emissions. Following a decline in 2020, emissions increased by 5%, returning to levels seen in 2017-2018 (IEA, 2023). In the wake of the MEPC80 meeting in August 2023, the International Maritime Organization (IMO) introduced the "2023 IMO strategy on reduction of greenhouse gas (GHG) emission for ships" updating emission

*Author to whom all correspondence should be addressed (e-mail: zhoujingmiao@dlufl.edu.cn).

reduction requirements: by 2030, international shipping must reduce annual carbon emissions by at least 20% to 30% compared to 2008 levels, and by 2040, this reduction should reach at least 70%, aiming for 80% (IMO, 2023). It is clearly a difficult task to achieve these ambitious carbon reduction targets. To accelerate this process, the maritime industry needs to promote low-carbon and zero-carbon fuels and technologies (CCS, 2023; DNV 2023).

The efforts to reduce emissions in international shipping primarily focus on three aspects: alternative fuels and power systems, technologies, and operations (ITF, 2018). The alternative fuels and power systems aspects involve the deployment of power systems and the application of alternative fuels. The technology aspect includes measures such as the use of light materials and slender hull design, while the operational aspect encompasses strategies such as slow steaming and adjusting ship size (ITF, 2018). In recent years, liquefied natural gas (LNG), methanol, ammonia, and hydrogen have emerged as feasible alternative fuels due to technological progress (Solakivi et al., 2022). However, changes related to engines, fuel tanks, and ship size result in a lower container capacity compared to traditional fuels, leading to a loss of useful space (Korberg et al., 2021; Lagemann et al., 2022). Among the various new power systems, dual-fuel (DF) engines offer the flexibility to accommodate various alternative fuels (MAN, 2021; Zhao et al., 2023). In addition, fuel cells (FC) represent another alternative fuel power system, distinct from battery-based systems, generating electricity by chemically converting fuel. The overview of alternative fuels and power systems is presented in **Table 1**. Still, there is a long way to go as alternative fuel uptake (excluding LNG and LPG) as part of the total world active fleet amounted to only 0.36% in ship numbers and 0.08% in gross ton capacity in early 2023 (UNCTAD, 2023).

Table 1. An overview of alternative fuels and power systems

| Alternative fuels/power systems | Development | Challenge |
|---|---|---|
| LNG [a] | LNG excels over other alternative fuels with its high technological maturity, comprehensive regulations, and high energy density. It represents 8.74% of the 15.96% of ship orders for alternative fuel power. | LNG contains carbon, which limits its ability to reduce $CO_2$ emissions significantly. Additionally, methane slip during usage can impact greenhouse gas emissions, adding further environmental concerns. |
| Methanol [b] | It is liquid at standard pressure, and easy to store and transport, requiring only minor modifications to ships and bunkering infrastructure for use in most ships' combustion engines. | The use of methanol as a fuel on ships introduces risks of flammability, toxicity, and issues such as corrosion and swelling. |
| Ammonia [c] | Ammonia, carbon-free and boasting an energy density comparable to methanol—double that of hydrogen—is easily liquefied and safely stored and transported, making it an ideal energy source. | Ammonia, with limited fuel use experience, has poor combustion properties, high self-ignition temperature, low flame speed, narrow flammability, and high evaporation heat. It also produces nitrogen oxide emissions. |
| Hydrogen [d] | Hydrogen, with the highest energy-to-weight ratio among alternative fuels, emits no $CO_2$, PM, or $SO_X$ when burned, making it a promising candidate for decarbonization. | Hydrogen's low volumetric energy density limits its use to small, short-range vessels, with unresolved safety concerns regarding fuel volatility. Gaseous hydrogen is liquefied by cooling it to below −253°C requiring expensive storage tanks onboard. |
| DF [e] | DFs are flexible, operating in liquid diesel or gas modes. In diesel mode, they function like standard engines, while gas mode supports lean combustion, reducing $NO_X$ emissions and boosting efficiency. | Although DFs have clear advantages in emissions, they can experience knocking under conditions of engine overload and high temperatures. |
| FC [f] | FCs offer enhanced fuel efficiency by directly converting chemical to electrical energy, with negligible emissions. Modular and more | FCs are not yet viable for large ocean-going ships due to limited power density, technological maturity, and cost-effectiveness. |

efficient than diesel engines at partial loads, they boost operational efficiency.

**Note:**

a. Solakivi et al. (2022); DNV (2024)
b. Solakivi et al. (2022); ITF (2018)
c. ITF (2018); CCS (2021)
d. Solakivi et al. (2022); ITF (2018); ABS (2019); CCS (2023)
e. Bui et al. (2022); Zou et al. (2021)
f. Sürer and Arat (2022); CCS (2023)

When it comes to ports, the key lies in the development of fuel bunkering facilities. So far, LNG bunkering facilities have witnessed the most extensive global expansion, with 158 ports worldwide equipped for LNG bunkering by 2023 (Clarksons, 2023a). In many cases, port authorities facilitated the development of such facilities to solve the chicken-and-egg conundrum towards LNG adoption in shipping (Wang and Notteboom, 2015; Ha et al., 2023). Methanol bunkering is also available, with the Port of Rotterdam initiating the world's first methanol bunkering barge operation (Waterfront Shipping, 2021), while other world ports are preparing for methanol-fueled vessels as exemplified by the 2023 MoU between Maersk and Shanghai International Port Group (SIPG) aiming at starting green methanol fuel vessel-to-vessel bunkering operations in 2024. Other alternative fuels, such as ammonia and hydrogen, are also gaining momentum, with Norway constructing the world's first ammonia bunkering facility (Azane Fuel Solutions, 2023). International shipping carbon reduction is poised for effective progress, anticipating substantial demand for alternative fuels and the capacity of most global ports to produce and store these fuels (Hydrogen Council, 2020; The Royal Society, 2020).

Container liner shipping, a vital sector of international shipping, accounts for 15% of the global maritime trade volume and over 70% of the total trade value (Liu et al., 2023; Xu et al., 2023, Clarksons, 2023b). By August 2023, the world boasted 6,006 fully cellular container ships, constituting about 18% of the world fleet's total deadweight tons and contributing to 31% of the entire shipping industry's carbon emissions (Clarksons, 2023c; Kramel et al., 2021). Despite fluctuations, the total volume of container trade within the Asian region has shown a steady upward trend over the years. Frequent container trade activities are expected to lead to increased emissions (Clarksons, 2023b). Cariou et al. (2019) found that a 33% $CO_2$ reduction in container shipping occurred between 2007 and 2016 in part because of an improved $CO_2$ fuel efficiency realized through slow steaming and technology change. These positive effects were slightly counterbalanced by an increase in the total fleet capacity deployed. In recent years, container carriers and shipowners have been placing massive newbuild orders for dual-fuel container ships combining methanol and very low sulfur fuel oil (VLSFO), or LNG and VLSFO.

Smaller container vessels operating on short sea and feeder routes deserve special attention in the decarbonization debate. Short sea routes are ideal testing grounds for future carbon reduction technologies. Short-sea ships can frequently call at ports and spend most of their time in environmentally controlled areas under local and regional regulations. This makes them well-suited for new technologies requiring specialized infrastructure and regulatory support, such as batteries and alternative fuels (ABS, 2019; EPRS, 2020). Indeed, a comparison of the percentages in Table 1 reveals that primarily smaller vessels operating on shorter routes are the first to have implemented battery/hybrid technology or the use of alternative fuels such as methanol. According to a report by UNCTAD, feeder container ships have higher carbon intensity compared to other types of container ships. Specifically, container ships with capacities of 1,000-1,999 TEU and 2,000-2,999 TEU have carbon intensities of approximately 20 grams and 15 grams of $CO_2$ per ton-mile, respectively (UNCTAD, 2022). As the size of the ships increases, the carbon intensity gradually decreases to around 8 grams per ton-mile. Larger ships consume less fuel per unit of cargo volume and thus emit less $CO_2$. Consequently, carbon reduction in liner shipping holds paramount significance, especially for feeder ships operating on short sea routes. Evolving business practices underline the key role short sea vessels will continue to play in the shipping decarbonization path. For example, the hub-feeder network configurations in container shipping heavily rely on shortsea and feeder operations, as exemplified by the proposed liner shipping network of the Gemini partnership between Maersk and Hapag Lloyd which is built around selected hub ports (Rahman, 2024). Over half of the 44 existing green shipping corridor initiatives globally focus on short sea routes (Global Maritime Forum, 2024). Green shipping corridors are specific trade routes where the feasibility of zero-emission shipping is catalyzed by public and private action. From a global trade perspective, nearshoring of global industrial activity will potentially boost regional shipping activity and the use of short sea operations (McKinsey & Company, 2017; US Chamber of Commerce, 2023). Policymakers have also developed a strategic interest in short sea shipping. For example, EU policymakers have assigned a strong role to short sea shipping in reaching the EU transport goal of reducing 60% of greenhouse gas emissions generated by transport by 2050, and the shift of 30% of road freight over 300 km to other modes by 2030. Thus, the study of decarbonization of container shipping operations on short sea routes is needed and justified.

This paper proposes a green liner shipping problem (GLSP) from the viewpoint of liner companies operating on short sea routes, integrating deployment of a heterogeneous green fleet, speed determination, and multiple fuel bunkering. The companies must make optimal decisions within their routine fixed route networks while meeting the transport volumes determined by pre-set service frequencies. Decisions must consider various factors such as the layout of fuel bunkering ports for different fuels and the prices at these ports, necessitating a careful balance between total operating costs and carbon emissions. Our study combines several key aspects. Firstly, we consider heterogeneous fleets. Prior research aimed to deploy heterogeneous fleets on fixed route networks to cope with uncertain cargo demands, mainly considering differences in characteristics such as capacity and ship age (Pasha et al., 2021; Wang and Wang, 2021). On this basis, our study incorporates the heterogeneity of carbon reduction technologies, highlighting the use of different ship types within the same route or across different service routes. These ships vary in terms of capacity, power systems, and the application of alternative fuels. Secondly, we differentiate at the level of fuel management. Prior studies primarily addressed the bunkering of a single fuel in ship operations (Liu et al., 2019; Zhao et al., 2022), while our research deals with heterogeneous fleets equipped with DF engines and FCs, involving multiple fuel bunkering scenarios, and not all ports have alternative fuels available. Typically, ship fuel consumption has speed as a key input (Wang and Meng, 2012). Lastly, our study considers multiple operational objectives. Extant literature mainly focused on cost control as the primary operational objective for liner companies (Sun et al., 2023). However, efficient carbon reduction is now a strategic goal for liner companies (Wang et al., 2023; Lagemann et al., 2022). The maritime industry has moved beyond treating environmental impacts as mere secondary constraints. The fast-changing regulatory framework on ship emissions at IMO and EU level as well as the pressure customers and society at large exert, make that environmental impact is no longer considered secondary to cost considerations. We aim to analyze how to make operational decisions that are both commercially viable and balance emission impact. The background of this research is illustrated in **Figure 1**. To our knowledge, this paper is a relatively novel effort, addressing the operational and managerial challenges of short-sea green container liner shipping at the strategic and tactical levels. It takes into account a scenario that is highly likely to become a reality within the next 5-10 years.

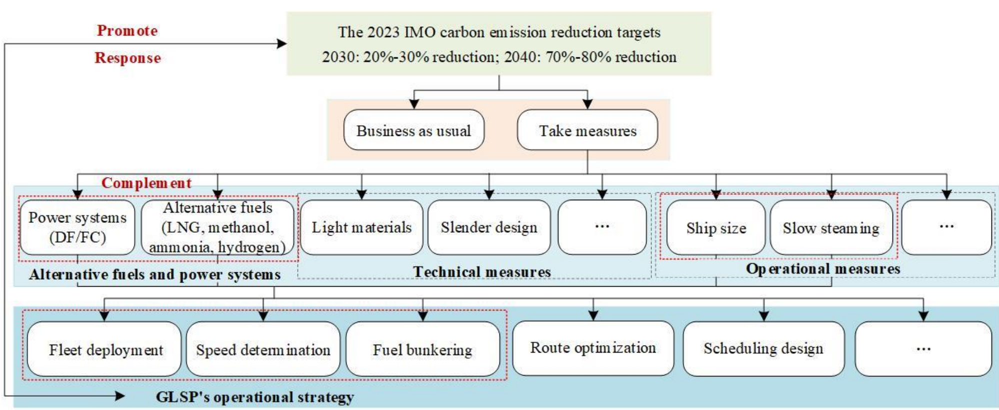


Figure 1. Green liner shipping problem (GLSP) operational strategy on short sea routes

This study holds value not only in theoretical research but also in practical business applications. The key envisaged contributions of this paper are as follows:

(1) For the GLSP problem, we introduce a bi-objective mixed-integer nonlinear programming model (BO-MINLP) that considers the use of power systems, alternative fuels, ship operational speeds, and ship sizes, and addresses the fact not all ports offer alternative fuels. This model incorporates inherent nonlinearity in the deployment

of heterogeneous fleets and the fuel consumption of ships on each route. It also addresses the tension between economic and carbon reduction objectives. The model builds upon prior work by Wu et al. (2022a) and Tan et al. (2020) to solve the problem of homogeneous fleet deployment with LNG DF technology on a single route.

(2) To solve the proposed BO-MINLP model, we undertake two approaches. Firstly, we linearize the model and transform the bi-objective problem into a single-objective one by applying the epsilon method. This adjustment enables us to obtain results using a commercial solver that implements the precise algorithm. Secondly, we develop a customized multi-objective genetic algorithm (MOGA) based on decision logic related to fleet deployment, speed determination, and fuel bunkering, and use it to solve the BO-MINLP. The effectiveness of these two approaches is verified through performance comparisons.

(3) To demonstrate the practical utility of the GLSP model and its associated algorithms, we develop an empirical application focusing on the short sea routes of SITC International Holdings Co., Ltd. (SITC). Through this application, we shed light on the delicate balance between economy and carbon reduction that liner companies are increasingly focused on. In addition, we offer specific decision-making references at the operational level.

The rest of this paper is structured as follows: Section 2 discusses the existing literature related to GLSP, Section 3 outlines the BO-MINLP model, Section 4 provides two algorithms for solving the model, Section 5 explores the effectiveness of the model and algorithms, and presents the case study results. The conclusion is provided in the final section.

## 2. Literature review

The issue of fleet deployment in liner shipping has been widely discussed within the academic community (Christiansen et al., 2013; Wang and Meng, 2017; Mollaoglu et al., 2023). However, as the shipping industry undergoes a green transformation and witnesses the ordering and deployment of large-scale container ships, there is a growing interest in the GLSP problem based on fleet deployment. In the context of heterogeneous fleet deployment, Wang and Wang (2021) studied the integrated optimization problem of deploying, sequencing, and scheduling heterogeneous fleets. They developed a mixed-integer programming model and customized a global optimization solution algorithm, surpassing the classical Branch & Cut algorithm. Furthermore, some scholars have extended their research by incorporating emission reduction technologies and emission impacts into GLSP. For instance, Wu et al. (2023) developed a mixed-integer non-linear programming (MINLP) model to determine the deployment of fleets while considering emission reduction technologies. Through linearization techniques, they transformed the nonlinear problem into a linear one and utilized commercial solvers to obtain results. Wang et al. (2023) addressed fleet deployment, speed optimization, cargo allocation, and compliance selection decisions under the impact of low-sulfur compliance requirements on carbon emissions in liner shipping. They proposed a two-stage model and designed a novel dual-population evolutionary algorithm to solve it. Pasha et al. (2021) delved into the decision-making of heterogeneous fleet deployment with integrated speed determination. They proposed an optimization model that considers emissions produced by liner shipping and designed a heuristic algorithm based on decomposition. To sum up, the above research mainly addressed fleet deployment in the context of either heterogeneous fleets' traditional functionalities or the integration of emission reduction technologies with homogeneous fleets. In contrast, this paper introduces a GLSP model that accounts for various capacities, power systems, and alternative fuels within a heterogeneous fleet.

The operational decisions related to this paper also include speed determination and fuel bunkering. Fuel management is a key concern for liner companies. De et al. (2023) proposed a two-stage analytical framework that combines game theory with optimization models to address the fuel bunkering problem for liner shipping, taking into account fuel price uncertainty. For example, Liu et al. (2019) investigated fuel bunkering and speed determination under uncertain freight demand. They developed a two-stage stochastic nonlinear programming model and compared various approaches to solve it. Previous research often integrated speed determination and fuel bunkering to address fuel management in liner shipping, but most of these approaches took the perspective of a homogeneous fleet and its operating cost. This paper not only seeks operational strategies that consider the balance between commercial value and emission impact but also accounts for various fuel bunkering requirements for heterogeneous fleets.

IMO's evolving carbon emission reduction targets have captured the attention of the shipping industry and academia. Research on ship operation management that incorporates carbon emission reduction has been gaining momentum. Ma et al. (2021) evaluated the carbon emissions of ships and introduced a MINLP to reorganize the sequence of port calls, route planning, speed determination, and fuel bunkering. They also designed an improved genetic algorithm that incorporates multiple encoding layers, pre-search, and tabu search to solve the model effectively. In a recent study, Tan et al. (2020) explored the optimization of fleet deployment, bunkering ports, bunkering volume, and speed determination for fleets employing LNG DF technology on major Asian routes. Wu et al. (2022a) constructed a MINLP and proposed operational strategies for fleet deployment, speed determination, and fuel bunkering utilizing LNG DF technology. The application of linearization techniques enabled problem-solving with the Gurobi solver. Furthermore, Wu et al. (2022b) extended their research to investigate the effects of speed, displacement, and voyage options on very low sulfur fuel oil (VLSFO) fuel consumption and the energy efficiency operational index (EEOI). They studied the integrated optimization of fleet deployment, voyage planning, and speed determination within a liner shipping network. They developed a bi-objective mixed-integer non-linear programming (BO-MINLP) and introduced a customized precise algorithm to address it. Wu et al. (2023) developed a nonlinear integer programming model to address the optimization problem of selecting multi-fuel engines. This model aims to optimally determine engine types, fleet deployment, fuel selection, and speed optimization.

This paper extends the work of Wu et al. (2022a) and Tan et al. (2020) from homogeneous fleet GLSP on single routes, considering not only route network and heterogeneous fleet but also the balance between operating cost and carbon emissions. This introduces a new challenge for the solution algorithm.

To shed light on the positioning and novelty of this research, **Table 2** compares this study with ten relevant representative literature sources. The comparison covers aspects such as model types, decision-making content, key factors, emission effects, and solution methods. Unlike any of the other listed studies, this paper presents a BO-MINLP model to solve the GLSP that integrates heterogeneous fleet deployment, speed determination, and fuel bunkering with a specific focus on short sea routes.

Table 2. Comparison with related studies

| Literature | Model | Decision-making content | Key factors | Emission effects | Solution methods |
|---|---|---|---|---|---|
| Wang and Wang (2021) | MINLP | FD: √<br>SD: √<br>Bunkering: × | HF: √<br>SN: ×<br>MPSAF: × | × | Customized global optimization algorithm |
| Wu et al. (2023) | MINLP | FD: √<br>SD: √<br>Bunkering: × | HF: √<br>SN: √<br>MPSAF: × | √ | Commercial solvers |
| Wang et al. (2023) | Two-stage programming model | FD: √<br>SD: √<br>Bunkering: × | HF: ×<br>SN: √<br>MPSAF: × | √ | Constrained bi-objective dual population evolutionary algorithm |
| Pasha et al. (2021) | MINLP | FD: √<br>SD: √<br>Bunkering: × | HF: √<br>SN: √<br>MPSAF: × | √ | Decomposition-based heuristic algorithm |
| De et al. (2023) | Two-stage programming model | FD: ×<br>SD: ×<br>Bunkering: √ | HF: ×<br>SN: √<br>MPSAF: × | √ | Approximation algorithm |
| Liu et al. (2019) | Two-stage stochastic nonlinear programming model | FD: ×<br>SD: √<br>Bunkering: √ | HF: ×<br>SN: √<br>MPSAF: × | × | SAA, SAA based on scenario reduction and an L-shape method |
| Wu et al. (2022b) | BO-MINLP | FD: √<br>SD: √<br>Bunkering: × | HF: ×<br>SN: √<br>MPSAF: × | √ | Customized precise algorithm |
| Ma et al. (2021) | MINLP | FD: ×<br>SD: √<br>Bunkering: √ | HF: ×<br>SN: ×<br>MPSAF: × | √ | Improved genetic algorithm |

| | | | | | |
|---|---|---|---|---|---|
| Tan et al. (2020) | MILP | FD: √<br>SD: √<br>Bunkering: √ | HF: ×<br>SN: ×<br>MPSAF: × | √ | Decomposition-based heuristic algorithm |
| Wu et al. (2022a) | MINLP | FD: √<br>SD: √<br>Bunkering: √ | HF: ×<br>SN: ×<br>MPSAF: × | √ | Gurobi |
| This paper | BO-MINLP | FD: √<br>SD: √<br>Bunkering: √ | HF: √<br>SN: √<br>MPSAF: √ | √ | Epsilon constraint method and customized multi-objective genetic algorithm |

**Note:**

a. MINLP represents mixed integer nonlinear programming; MILP represents mixed integer linear programming; BO-MINLP represents bi-objective mixed integer nonlinear programming.

b. FD represents fleet deployment.

c. SD represents speed determination.

d. HF represents heterogeneous fleet.

e. SN represents the shipping network.

f. MPSAF represents multiple power systems and alternative fuels.

g. √ indicates that the element is considered, while × indicates that it is not considered.

## 3. Problem description, assumptions, and model construction

### *3.1. Problem description*

The research problem of GLSP can be described as:

Liner companies operate a heterogeneous fleet consisting of container ships with variations in their power system configurations (denoted as $k \in K$), the application of alternative fuels (denoted as $f \in F^A$), and cargo hold capacities (denoted as $v \in V$). The compatibility among these factors on a given container ship is represented by $\xi_{vkf}$ (Zhao et al., 2024). In this heterogeneous fleet, ships can be deployed on liner services serving the same or different routes. The number of container ships with a specific power system $k$, applied alternative fuel $f$, and cargo capacity type $v$ available is denoted as $m_{vkf}$. The matching between these container ships and fossil fuel $f'$ is denoted as $\gamma_{vkff'}$. These container ships are categorized into two groups: DF ships $K^{DF}$ requiring the combustion of both fossil fuel $F^F$ and alternative fuel $F^A$, and FC ships $K^{FC}$ solely relying on alternative fuel $F^A$. Different fuel types $f \in F$ are associated with distinct carbon emission factors $E_f$ and low calorific values $L_f$. Low calorific value refers to the energy released during fuel combustion.

Liner companies typically operate multiple routes, and the set of routes $R$ comprises a given route network (Wang et al., 2023). Each route $r$ is characterized by a fixed order of port calls $i$ where the distance between two successive call ports $i$ and $i+1$ is referred to as a leg $i$. The length of leg $i$ on route $r$ is denoted as $d_{ri}$. Within this predefined route network, the liner fleet must provide services at a specified frequency $\phi_r$ to fulfill the volume of freight transported $q_{ri}$ at all ports on each route. It is worth noting that the typical frequency on the main trade routes is a weekly departure. However, each ship must not exceed its cargo hold capacity $Q^C_{vkf}$. It is worth noting that the capacity of reefer slots and their impact on fuel consumption, as well as the loss of cargo hold capacity due to the different storage tank capacities required for alternative fuels, are not considered in our study. Given the diversity in the fleet, container ships of different ship types $\{v,k,f\}$ on various routes $r$ incur different fixed ship costs $C_{rvkf}$, which include capital costs, crew wages, insurance premiums, and so on (Wang and Wang, 2021; Wu et al., 2023).

Container ships have the flexibility to set their sailing speed $s \in S$ on different legs. And the optimal speed for deploying ships with varying container capacities, engine configurations, and fuel consumption rates on the same leg is unique (Pasha et al., 2021). Consequently, the alternative fuel consumption $\beta^{A}_{rivkf}$ and matching fossil fuel consumption $\beta^{F}_{rivkff'}$ for container ships when sailing on each leg are mainly influenced by the sailing power requirement $M_{vks}$, the required sailing time $T_{ris}$, and the optimal sailing speed $w_{ris}$, which needs to be determined. Moreover, all ships burn alternative fuels while at port (note that there still is scarce availability of onshore power supply (OPS) solutions for container vessels in world ports), and their fuel consumption is linked to the port calling time $T_{ri}$ and the ship's fuel consumption rate $F_{vkf}$ in port (Zhao et al., 2023; Zhao et al., 2024).

For DF ships, the fuel inventory level must not exceed the tank capacity $Q^{A}_{vkf}$ and $Q^{F}_{vkff'}$ for both alternative fuel and fossil fuel. Similarly, FC ships must remain within their tank capacity $Q^{A}_{vkf}$. However, these ships must maintain sufficient fuel levels to support the energy consumption required for sailing on the leg $i$ of the route $r$ (Tan et al. 2020). Otherwise, container ships need to bunker fuel at a specified bunkering port $z_{if}$, which can provide the required fuel $f$, ensuring they can complete their service on route $r$. The price of fuel at the bunkering port is represented as $C_{if}$.

In light of the above, the GLSP, which centers on heterogeneous fleet deployment, speed determination, and fuel bunkering, involves the following decision variables: the number of container ships with power system $k$ and applied alternative fuel $f \in F^{A}$ of cargo capacity type $v$ deployed on route $r$; the consumption $\beta^{A}_{rivkf}$ of alternative fuel $f \in F^{A}$ and the consumption $\beta^{F}_{rivkff'}$ of fossil fuel $f' \in F^{F}$ of different types container ships $\{v, k, f\}$ when sailing on leg $i$ of route $r$. These container ships are equipped with alternative fuel $f \in F^{A}$ at an inventory level of $\pi^{A}_{rivkf}$, fossil fuel $f' \in F^{F}$ at an inventory level of $\pi^{F}_{rivkff'}$. The decision to bunker and the corresponding fuel bunkering volumes are denoted as $\alpha^{A}_{rivkf}$ and $\alpha^{F}_{rivkff'}$ when the ships call at port $i$.

It is important to note that these decisions are made within the context of liner companies' long-term strategies, which aim to strike a balance between economic competitiveness and carbon emission reduction. A simple example of the GLSP is presented in **Figure 2**.

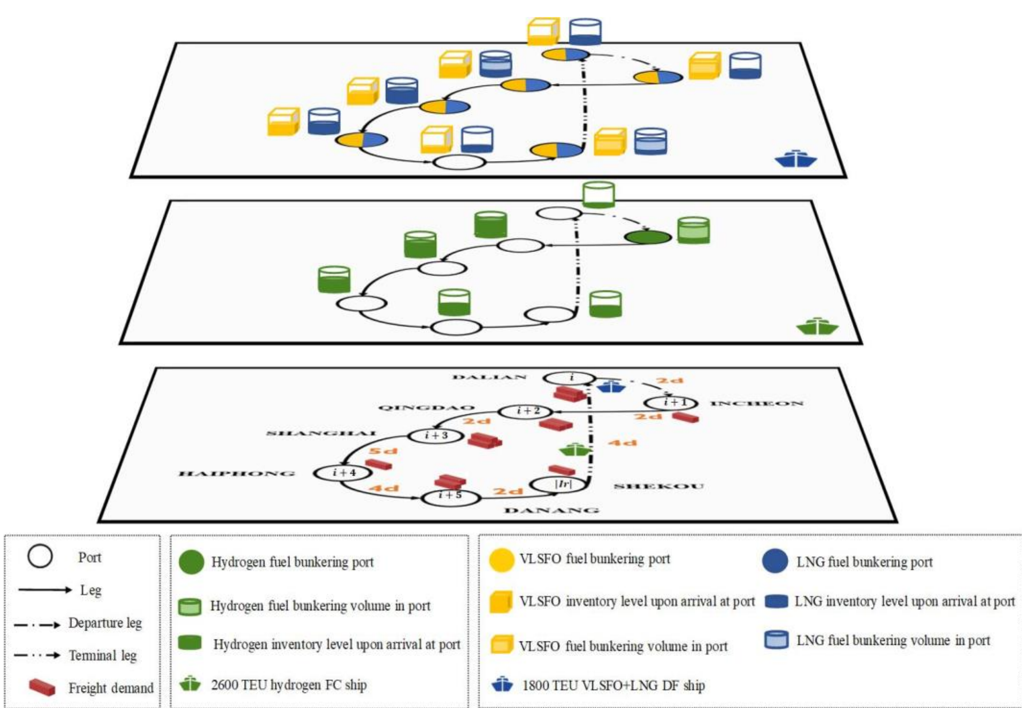

Figure 2. A simple example of GLSP

**Note:** This figure shows a feasible example of fleet deployment, speed determination, and fuel bunkering on an intra-Asian container liner service connecting northeastern China and the Republic of Korea with southern China and Vietnam. Other routes and ship types are also considered in this paper.

### *3.2. Assumptions*

This study makes the following assumptions.

**Assumption 1**

The liner service route and port of call sequence are known and fixed, forming a closed loop in practice, with a service frequency of once per week (Wang et al., 2023).

**Assumption 2**

Using different ship types within the same or across different service routes (Wang and Wang, 2021; Pasha et al., 2021). These ships vary in capacity, power systems, and the application of alternative fuels.

**Assumption 3**

Given that the investment cost differences for ships with different power systems and alternative fuels have already been considered, it is assumed that ships with different power systems and alternative fuels can have the same container capacity (Wu et al., 2023; Zhao et al., 2023; Zhao et al., 2024).

**Assumption 4**

Ships consume only alternative fuels while berthed at ports (Zhao et al., 2023; Zhao et al., 2024).

### *3.3. Symbol description*

Before proposing the mathematical model, we define the indexes, sets, parameters, and decision variables involved in GLSP, as shown in **Table 3**.

Table 3. Model symbol and description

| **Set** | **Description** |
|---|---|
| $R$ | Set of routes, indexed by $r$ |
| $I_r$ | Set of call ports (legs) on the route $r$, indexed by $i$. The index $i$ also represents the leg from $i$ to $i+1$. $\lvert I_r \rvert$ is the last call port before returning to the departure port. |
| $K$ | Set of power systems, indexed by $k$ |
| $K^{DF} \subseteq K$ | Subset of DF power systems |
| $K^{FC} \subseteq K$ | The subset of FC power systems, $K^{FC} = K - K^{DF}$ |
| $V$ | Cargo hold capacity, indexed by $v$ |
| $F$ | Set of applied fuels, indexed by $f$ or $f'$ |
| $F^F \subseteq F$ | The subset of fossil fuels. This paper focuses on the fossil fuel VLSFO. |
| $F^A \subseteq F$ | The subset of alternative fuels includes MGO, LNG, ammonia, hydrogen, and methanol. Due to the necessity for dual-fuel vessels to accommodate two types of fuels—one being the conventional fossil fuel VLSFO and the other a cleaner alternative fuel to comply with environmental regulations, this study includes the cleaner fossil fuel MGO in the set of alternative fuels to facilitate the differentiation of dual fuels, $F^A = F - F^F$ |
| $S$ | Set of speeds, indexed by $s$ |
| **Parameter** | **Description** |
| $m_{vkf}$ | The available quantity of type $v$ container ships with power system $k$ and alternative fuel $f \in F^A$ |
| $Q^C_{vkf}$ | The cargo hold capacity of type $v$ container ships with power system $k$ and alternative fuel $f \in F^A$ (TEU) |
| $Q^A_{vkf}$ | The storage tank capacity for alternative fuel $f \in F^A$ of type $v$ container ships with power system $k$ and alternative fuel $f \in F^A$ (T) |
| $Q^F_{vkff'}$ | The storage tank capacity for fossil fuel $f' \in F^F$ of type $v$ container ship with power system $k$ and alternative fuel $f \in F^A$ (T) |
| $C_{if}$ | The price of fuel $f$ in port $i$ (USD) |
| $q_{ri}$ | The volume of freight transported of the port $i$ on route $r$ (TEU) |

| | |
|---|---|
| $C_{rvkf}$ | The fixed ship cost of type $v$ container ships with power system $k$ and alternative fuel $f \in F^A$ on route $r$ (fixed ship cost for completing a voyage) (USD) |
| $D_{ri}$ | The sailing distance of the leg $i$ on route $r$ (NM) |
| $T_{ris}$ | The sailing time of leg $i$ at speed $s$ on route $r$ (H), $T_{ris} = D_{ri}/s$ |
| $T_{ri}$ | The calling time of the ship at port $i$ on route $r$ (H) |
| $F_{vkf}$ | The fuel consumption rate at the port of type $v$ container ships with power system $k$ and alternative fuel $f \in F^A$, where only alternative fuels are consumed |
| $E_f$ | The carbon emission factor of fuel $f$ (T/T) |
| $L_f$ | The low calorific value of fuel $f$ (MJ/T) |
| $M_{vks}$ | The hourly sailing power requirement of type $v$ container ships with power system $k$ (MJ/T) |
| $\phi_r$ | The port service frequency of route $r$ (Day), which is set to 7 days corresponding to a weekly liner service |
| $z_{if}$ | Whether the port $i$ is the bunkering port for fuel $f$ |
| $\xi_{vkf}$ | The matching of power system $k$, alternative fuel $f \in F^A$, and cargo hold capacity $v$ on the same container ship |
| $\gamma_{vkff'}$ | The compatibility of container ships with power system $k$, alternative fuel $f \in F^A$, and cargo hold capacity $v$ with fossil fuel $f'$ |
| **Decision variable** | **Description** |
| $\alpha^A_{rivkf}$ | The fuel bunkering amount of alternative fuel $f \in F^A$ for type $v$ container ships with power system $k$ and alternative fuel $f \in F^A$ in port $i$ of route $r$ |
| $\alpha^F_{rivkff'}$ | The fuel bunkering amount of fossil fuel $f' \in F^F$ for type $v$ container ships with power system $k$ and alternative fuel $f \in F^A$ on port $i$ of route $r$ |
| $\beta^A_{rivkf}$ | The fuel consumption amount of alternative fuel $f \in F^A$ for type $v$ container ships with power system $k$ and alternative fuel $f \in F^A$ at port $i$ of route $r$ |
| $\beta^F_{rivkff'}$ | The fuel consumption amount of fossil fuel $f' \in F^F$ or type $v$ container ships with power system $k$ and alternative fuel $f \in F^A$ on port $i$ of route $r$ |
| $\pi^A_{rivkf}$ | The inventory level of alternative fuel $f \in F^A$ for type $v$ container ships with power system $k$ and alternative fuel $f \in F^A$ on port $i$ of route $r$ |
| $\pi^F_{rivkff'}$ | The fuel inventory level of fossil fuel $f' \in F^F$ for type $v$ container ships with power system $k$ and alternative fuel $f \in F^A$ on port $i$ of route $r$ |
| $w_{ris}$ | Whether the ship sails in leg $i$ at speed $s$ on route $r$ |
| $x_{rvkf}$ | The number of type $v$ container ships with power system $k$ and alternative fuel $f \in F^A$ deployed on the route $r$ |

*3.4. Model construction*

*3.4.1. Bi-objective function*

$$\begin{aligned}\min C = &\sum_{r\in R}\sum_{i\in I_r}\sum_{v\in V}\sum_{k\in K}\sum_{f\in F^A} C_{rvkf}x_{rvkf} + \sum_{r\in R}\sum_{i\in I_r}\sum_{v\in V}\sum_{k\in K}\sum_{f\in F^A} C_{if}\alpha^A_{rivkf}x_{rvkf} \\ &+ \sum_{r\in R}\sum_{i\in I_r}\sum_{v\in V}\sum_{k\in K^{DF}}\sum_{f\in F^A}\sum_{f'\in F^F} C_{if'}\alpha^F_{rivkff'}x_{rvkf}\end{aligned} \tag{1}$$

$$\begin{aligned}\min E = &\sum_{r\in R}\sum_{i\in I_r}\sum_{v\in V}\sum_{k\in K}\sum_{f\in F^A} E_f\beta^A_{rivkf}x_{rvkf} + \sum_{r\in R}\sum_{i\in I_r}\sum_{v\in V}\sum_{k\in K}\sum_{f\in F^A}\sum_{f'\in f^F} E_{f'}\beta^F_{rivkff'}x_{rvkf} \\ &+ \sum_{r\in R}\sum_{i\in I_r}\sum_{v\in V}\sum_{k\in K}\sum_{f\in F^A} E_f F_{vkf}T_{ri}x_{rvkf}\end{aligned} \tag{2}$$

Objective (1) aims to minimize the total operating cost for completing a single voyage within a given route network using a heterogeneous fleet. The total operating cost includes both fixed ship costs and variable fuel bunkering costs. It is worth noting that here we assume fuel bunker is only a variable cost and is not included in fixed ship cost. Meanwhile, Objective (2) focuses on minimizing total carbon emissions, accounting for emissions during sea voyages and port calls.

*3.4.2. Constraints*

$$\sum_{s\in S} w_{ris} = 1, i \in I_r, r \in R \tag{3}$$

$$\sum_{i\in I_r} q_{ri} \le \sum_{v\in V}\sum_{k\in K}\sum_{f\in F^A} Q^C_{vkf} x_{rvkf}, r \in R \tag{4}$$

$$24\sum_{v\in V}\sum_{k\in K}\sum_{f\in F^A} \phi_r x_{rvkf} \ge \sum_{i\in I_r}\sum_{s\in S} T_{ris} w_{ris} + \sum_{i\in I_r} T_{ri}, r \in R \tag{5}$$

$$\xi_{vkf} L_f \beta^A_{rivkf} + \gamma_{vkff'} L_{f'} \beta^F_{rivkff'} = \sum_{s\in S} \xi_{vkf} M_{vks} T_{ris} w_{ris}, f' \in F^F, f \in F^A, k \in K^{DF}, v \in V, i \in I_r, r \in R \tag{6}$$

$$\gamma_{vkff'} L_{f'} \beta^F_{rivkff'} \ge 0.03 \sum_{s\in S} \gamma_{vkff'} M_{vks} T_{ris} w_{ris}, f' \in F^F, f \in F^A, k \in K^{DF}, v \in V, i \in I_r, r \in R \tag{7}$$

$$\xi_{vkf} L_f \beta^A_{rivkf} = \sum_{s\in S} \xi_{vkf} M_{vks} T_{ris} w_{ris}, f \in F^A, k \in K^{FC}, v \in V, i \in I_r, r \in R \tag{8}$$

$$\xi_{vkf} \alpha^A_{rivkf} \le \xi_{vkf} z_{if} (Q^A_{vkf} - \pi^A_{rivkf}), f \in F^A, k \in K, v \in V, i \in I_r, r \in R \tag{9}$$

$$\xi_{vkff'} \alpha^F_{rivkff'} \le \xi_{vkff'} z_{if'} (Q^F_{vkff'} - \pi^F_{rivkff'}), f' \in F^F, f \in F^A, k \in K^{DF}, v \in V, i \in I_r, r \in R \tag{10}$$

$$\xi_{vkf} \pi^A_{rivkf} = \xi_{vkf} (\pi^A_{r|I_r|vkf} + \alpha^A_{r|I_r|vkf} - \beta^A_{r|I_r|vkf} - F_{vkf} T_{r|I_r|}), f \in F^A, k \in K, v \in V, i \in I_r : i = 1, r \in R \tag{11}$$

$$\xi_{vkff'} \pi^F_{rivkff'} = \xi_{vkff'} (\pi^F_{r|I_r|vkf} + \alpha^F_{r|I_r|vkf} - \beta^F_{r|I_r|vkf}), f' \in F^F, f \in F^A, k \in K^{DF}, v \in V, i \in I_r : i = 1, r \in R \tag{12}$$

$$\xi_{vkf} \pi^A_{ri+1vkf} = \xi_{vkf} (\pi^A_{rivkf} + \alpha^A_{rivkf} - \beta^A_{rivkf} - F_{vkf} T_{ri}), f \in F^A, k \in K, v \in V, i \in I_r : i < |I_r|, r \in R \tag{13}$$

$$\xi_{vkff'} \pi^F_{ri+1vkff'} = \xi_{vkff'} (\pi^F_{rivkf} + \alpha^F_{rivkf} - \beta^F_{rivkf}), f' \in F^F, f \in F^A, k \in K^{DF}, v \in V, i \in I_r : i < |I_r|, r \in R \tag{14}$$

$$\sum_{r\in R} x_{rvkf} \le m_{vkf}, f \in F^A, k \in K, v \in V \tag{15}$$

$$\alpha^A_{rivkf}, \beta^A_{rivkf}, \pi^A_{rivkf} \ge 0, f \in F^A, k \in K, v \in V, i \in I_r, r \in R \tag{16}$$

$$\alpha^F_{rivkff'}, \beta^F_{rivkff'}, \pi^F_{rivkff'} \ge 0, f' \in F^F, f \in F^A, k \in K^{DF}, v \in V, i \in I_r, r \in R \tag{17}$$

$$x_{rvkf} \in Z^+ \cup \{0\}, f \in F^A, k \in K, v \in V, r \in R \tag{18}$$

$$w_{ris} \in \{0,1\}, v \in V, s \in S, i \in I_r : i < |I_r|, r \in R \tag{19}$$

Constraint (3) ensures that each leg has a unique selected speed, while Constraint (4) guarantees that the volume of freight transported does not exceed the cargo hold capacity of the deployed fleet. Constraint (5) maintains a minimum service frequency for ships on each route. Constraint (6) defines the energy formula that must be met for fuel combustion in DF ships, and Constraint (7) specifies the corresponding energy formula for fossil fuels used as pilot oil in DF ships (Tan et al. 2020). Constraint (8) outlines the energy formula that must be satisfied for fuel combustion in FC ships. Constraints (9) and (10) are prerequisites, indicating that fuel can only be bunkered in ports designed for such purposes and ships must consume the specific fuel they bunkered. Constraints (11) and (12) define the initial fuel inventory levels for ships departing from their departure ports, while Constraints (13) and (14) specify the mandatory fuel inventory levels at all ports except the departure port. Constraint (15) governs the number of ships deployed, and Constraints (16)-(19) specify the allowable ranges for decision variables, including fossil fuel bunkering, fossil fuel consumption, fossil fuel inventory levels, alternative fuel bunkering, alternative fuel consumption, alternative fuel inventory levels, number of deployed container ships and speed of the ship sails in leg.

For a type $v$ container ship with power system $k$, the hourly sailing power requirement $M_{vks}$ (MJ/T), i.e., the demand for fuel consumption, can be calculated by:

$$M_{vks} = p_{vk} \left(s/s_{vk}\right)^n 3.6/\eta_{vk}, k \in K, v \in V \tag{20}$$

where, $p_{vk}$ is the reference power of type $v$ container ship with power system $k$ at the design speed $s_{vk}$; $n$ =3 is the index of the relationship between speed and power (Tan et al., 2020); $\eta_{vk}$ is the fuel combustion efficiency of the type $v$ container ship with power system $k$. Since DF ships and FC ships also burn fuel, the same formula is adopted for combustion energy.

## 4. Solution method

There are generally two types of methods for solving multi-objective problems: one is to use weighting methods or the epsilon constraint method to convert a bi-objective problem into a series of single-objective problems and then find multiple solutions for these single-objective problems to obtain the Pareto optimal set (Zhen et al., 2020). The other is to use hybrid heuristic, metaheuristic, and hyperheuristic algorithms to approximate the Pareto frontier of multi-objective problems, which are popular in recent studies (Wang et al., 2023; Nunes et al., 2023). While genetic algorithms are not considered the most cutting-edge heuristic method, they are still notably effective. Particularly suited for multi-objective optimization, genetic algorithms generate multiple solutions, helping to identify non-inferior solutions in multi-objective optimization scenarios (Basnet and Weintraub, 2009).

In the context of our BO-MINLP formulated for GLSP, we apply the epsilon constraint method and a customized MOGA respectively. Due to the presence of continuous variable multiplication and overly strict constraints in our BO-MINLP, preprocessing is necessary before utilizing these methods. The Pareto solution sets produced by these two approaches are then subjected to fuzzy decision-making to rank the selected solutions based on the decision-maker's preferences, thus obtaining the best solution.

### *4.1. Epsilon constraint method*

#### *4.1.1. Linearization of bi-objective problem*

The objective functions (1) and (2) involve four continuous variables, namely $\alpha_{rivkf}^{A} x_{rvkf}$, $\alpha_{rivkff'}^{F} x_{rvkf}$, $\beta_{rivkf}^{A} x_{rvkf}$ and $\beta_{rivkff'}^{F} x_{rvkf}$, being multiplied, making them challenging to solve using precise linearization methods in certain cases. Although nonlinear models can be solved by general solvers under specific conditions, we choose to simplify the problem and improve solution efficiency by jointly discretizing the type of cargo hold capacity of the ship with the available ship quantity.

According to this capacity, we convert $x_{rvkf}$ into a binary 0-1 variable, where 1 signifies that type $v$ ship with the power system $k \in K$ and alternative fuel $f \in F^{A}$ is deployed on the route $r$, while 0 implies no deployment. Furthermore, we linearize the model using the Big-M method.

Introducing variable $n_{rivkf}$:

$$n_{rivkf} = \alpha_{rivkf}^{A} x_{rvkf}, \; f \in F^{A}, k \in K, v \in V, i \in I_r, r \in R \tag{21}$$

$$n_{rivkf} \le M_1 x_{rvkf}, \; f \in F^{A}, k \in K, v \in V, i \in I_r, r \in R \tag{22}$$

$$n_{rivkf} \le \alpha_{rivkf}^{A}, \; f \in F^{A}, k \in K, v \in V, i \in I_r, r \in R \tag{23}$$

$$n_{rivkf} \ge \alpha_{rivkf}^{A} x_{rvkf} - M_1 \left(1 - x_{rvkf}\right), \; f \in F^{A}, k \in K, v \in V, i \in I_r, r \in R \tag{24}$$

$$n_{rivkf} \in R^{+} \cup \{0\}, \; f \in F^{A}, k \in K, v \in V, i \in I_r, r \in R \tag{25}$$

Introducing variable $o_{rivkff'}$:

$$o_{rivkf} = \alpha_{rivkff'}^{F} x_{rvkf}, \; f' \in F^{F}, \; f \in F^{A}, k \in K^{DF}, v \in V, i \in I_r, r \in R \tag{26}$$

$$o_{rivkff'} \le M_1 x_{rvkf}, \; f' \in F^{F}, \; f \in F^{A}, k \in K^{DF}, v \in V, i \in I_r, r \in R \tag{27}$$

$$o_{rivkff'} \le \alpha_{rivkff'}^{F}, \; f' \in F^{F}, \; f \in F^{A}, k \in K^{DF}, v \in V, i \in I_r, r \in R \tag{28}$$

$$o_{rivkff'} \ge \alpha_{rivkff'}^{F} - M_1 \left(1 - x_{rvkf}\right), \; f' \in F^{F}, \; f \in F^{A}, k \in K^{DF}, v \in V, i \in I_r, r \in R \tag{29}$$

$$o_{rivkff'} \in R^{+} \cup \{0\}, \; f' \in F^{F}, \; f \in F^{A}, k \in K^{DF}, v \in V, i \in I_r, r \in R \tag{30}$$

Introducing variable $p_{rivkf}$:

$$p_{rivkf} = \beta_{rivkf}^{A} x_{rvkf}, \; f \in F^{A}, k \in K, v \in V, i \in I_r, r \in R \tag{31}$$

$$p_{rivkf} \le M_2 x_{rvkf},\ f \in F^A, k \in K, v \in V, i \in I_r, r \in R \tag{32}$$

$$p_{rivkf} \le \beta^A_{rivkf},\ f \in F^A, k \in K, v \in V, i \in I_r, r \in R \tag{33}$$

$$p_{rivkf} \ge \beta^A_{rivkf} - M_2\left(1 - x_{rvkf}\right),\ f \in F^A, k \in K, v \in V, i \in I_r, r \in R \tag{34}$$

$$p_{rivkf} \in R^+ \bigcup \{0\},\ f \in F^A, k \in K, v \in V, i \in I_r, r \in R \tag{35}$$

Introducing variable $u_{rivkff'}$:

$$u_{rivkff'} = \beta^F_{rivkff'} x_{rvkf},\ f' \in F^F,\ f \in F^A, k \in K^{DF}, v \in V, i \in I_r, r \in R \tag{36}$$

$$u_{rivkff'} \le M_2 x_{rvkf},\ f' \in F^F,\ f \in F^A, k \in K^{DF}, v \in V, i \in I_r, r \in R \tag{37}$$

$$u_{rivkff'} \le \beta^F_{rivkff'},\ f' \in F^F,\ f \in F^A, k \in K^{DF}, v \in V, i \in I_r, r \in R \tag{38}$$

$$u_{rivkff'} \ge \beta^F_{rivkff'} - M_2\left(1 - x_{rvkf}\right),\ f' \in F^F,\ f \in F^A, k \in K^{DF}, v \in V, i \in I_r, r \in R \tag{39}$$

$$u_{rivkff'} \in R^+ \bigcup \{0\},\ f' \in F^F,\ f \in F^A, k \in K^{DF}, v \in V, i \in I_r, r \in R \tag{40}$$

The value of M in the model can be set according to the practice. A too small value of M would fail to serve the purpose of linearization, while an excessively large value may cause constraint failure due to the accuracy of numerical calculations. In this model, the value of M does not need to be too large, and a value greater than the fuel storage tank capacity will suffice. We set M1 = M2 = 1850 according to the fuel storage tank capacity of the case study. As a result, the original model can be transformed as follows:

$$\begin{aligned} \min C = & \sum_{r\in R}\sum_{i\in I_r}\sum_{v\in V}\sum_{k\in K}\sum_{f\in F^A} C_{rvkf}\, x_{rvkf} + \sum_{r\in R}\sum_{i\in I_r}\sum_{v\in V}\sum_{k\in K}\sum_{f\in F^A} C_{if}\, n_{rivkf} \\ & + \sum_{r\in R}\sum_{i\in I_r}\sum_{v\in V}\sum_{k\in K^{DF}}\sum_{f\in F^A}\sum_{f'\in F^F} C_{if'}\, o_{rivkff'} \end{aligned} \tag{41}$$

$$\begin{aligned} \min E = & \sum_{r\in R}\sum_{i\in I_r}\sum_{v\in V}\sum_{k\in K}\sum_{f\in F^A} E_f\, p_{rivkf} + \sum_{r\in R}\sum_{i\in I_r}\sum_{v\in V}\sum_{k\in K}\sum_{f\in F^A}\sum_{f'\in f^F} E_{f'} u_{rivkff'} \\ & + \sum_{r\in R}\sum_{i\in I_r}\sum_{v\in V}\sum_{k\in K}\sum_{f\in F^A} E_f\, F_{vkf}\, T_{ri}\, x_{rvkf} \end{aligned} \tag{42}$$

s.t. (3)-(20), (21)-(40).

*4.1.2. Solving with the epsilon constraint method*

This paper employs the two-stage epsilon constraint method proposed by Zhen et al. (2020). Initially, the BO-MINLP is divided into two sub-problems. Sub-problem 1 sets the minimization of total operating cost as its objective and the total carbon emissions as the constraint. Sub-problem 2, conversely, takes the minimization of total carbon emissions as its objective, while employing the total operating cost as the constraint. The two sub-problems can be defined as follows:

$$\min\left\{C(x) \middle| E(x) \le \varepsilon, x \in X\right\} \tag{43}$$

$$\min\left\{E(x) \middle| C(x) \le \varepsilon, x \in X\right\} \tag{44}$$

where, $x$ is the decision vector of all decision variables; $\varepsilon$ falls within a specified range. First, the ideal points $(f_1^I, f_2^I)$ and the farthest points $(f_1^N, f_2^N)$ of the two subproblems are determined by solving the following single-objective problems:

$$f_1^I = \min\left\{C(x) \middle| x \in X\right\} \tag{45}$$

$$f_2^I = \min\left\{E(x) \middle| x \in X\right\} \tag{46}$$

$$f_1^N = \min\left\{C(x) \middle| E(x) = f_2^I, x \in X\right\} \tag{47}$$

$$f_2^N = \min\left\{E(x) \middle| C(x) = f_1^I, x \in X\right\} \tag{48}$$

Subsequently, solving (45)-(46) and (47)-(48) yields the lower and upper bounds for both objective functions, generating the approximate ideal points and the farthest points. The value range $[f_2^I, f_2^N]$ for $\varepsilon$ is thus determined. Further, by setting the step size $\Delta$, we derive specific values for $\varepsilon$, forming a series of single-objective problems. Solving these problems results in the Pareto solution set.

Each linear membership function for the Pareto objective functions can be given by:

$$\gamma_j\left(f_j^S\right) = \begin{cases} 1 & f_j^S \le f_j^I \\ \dfrac{f_j^N - f_j^S}{f_j^N - f_j^I} & f_j^I < f_j^S < f_j^N,\ j = 1,2; 1 \le s \le S \\ 0 & f_j^S \ge f_j^N \end{cases} \tag{49}$$

where, $\gamma_j\left(f_j^S\right)$ is the membership of objective function $j$ of solution $s$; $f_j^I$ and $f_j^N$ are the lower and upper bounds of objective function $j$, respectively; $f_j^s$ is objective function $j$ of solution $s$. The total membership $\theta^S$ can be calculated by:

$$\theta^S = \sum_{j=1}^{2} \omega_j \theta_j\left(f_j^S\right) \tag{50}$$

where, $\omega_j$ is the weight of objective function $j$; $\sum_{j=1}^{2} \omega_j = 1$ is determined by the decision maker regarding their preferences in terms of economic and environmental factors. The optimal solution corresponds to the solution with the highest $\theta^S$.

*4.2. Multi-objective genetic algorithm (MOGA)*

*4.2.1. Encoding and initialization*

Each route in our study forms a closed loop, originating from the departure port and eventually returning to the same starting point. An interesting challenge arises when configuring the initial fuel inventory level of the ship at the departure port. This setting significantly impacts the final solution, yet its precise value is elusive. Therefore, we opt not to assign an initial value to it. In addition, the calculation formula for this parameter, as defined by constraints (11)-(12), faces difficulties when incorporated into the MOGA framework. To expedite the generation of the initial feasible solution, we relax constraints (11)-(12) and compute the fuel bunkering volume for the ship at the departure port as a substitute for setting the initial inventory level. It is worth noting that the fuel inventory level upon the ship's return to the departure port need not strictly match the level at departure.

Given that ship speed has a major impact on fuel consumption, fuel bunkering, fuel inventory level, and fleet deployment, we break down the original problem into distinct stages. Since our legs are predefined, we first determine the optimal speed for each leg, ensuring the effective implementation of constraint (3). Subsequently, we calculate the required fuel bunkering and fuel consumption, along with the corresponding fuel inventory level. In fact, the primary drivers for fuel bunkering decisions are the fuel prices at different ports and the fuel inventory level of the ship. As speed influences the fuel consumption of the ship, thereby affecting the ship's fuel inventory level, it indirectly impacts fuel bunkering decisions. Finally, we resolve the fleet deployment strategy.

The original problem is segmented into subproblems requiring repetitive deployment of the GA. The two decision variables, speed, and fuel bunkering, are subject to encoding. We adopt gray coding for each decision variable to achieve better variation properties between the encoded and corresponding decoded values, as illustrated in **Figure 3** (Sarker et al., 2001).

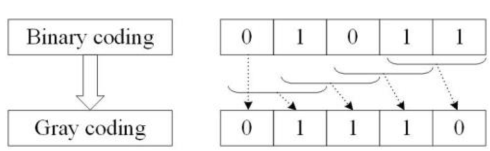

Figure 3. Conversion between Gray coding and binary coding

Because speed and fuel bunkering are calculated based on legs, we assume that each chromosome is made up of $\sum_{r \in R} |I_r|$ genes, i.e., the total number of legs in the route network. Please note that when a ship navigates a predefined route that includes a specific leg twice, these occurrences are considered as two separate legs. Here, the initial population is generated randomly. During decoding, we convert the generated binary values into their decimal counterparts.

*4.2.2. Crossover*

The algorithm employs the widely-used single-point crossover mechanism, wherein two individual chromosomes are recombined to yield two new chromosomes.

*4.2.3. Mutation*

For mutation, a bit-flipping strategy is employed. This involves randomly selecting several genes within specific chromosomes and inverting their values.

*4.2.4. Fast non-dominated sorting*

Our algorithm adopts the fast non-dominated sorting genetic algorithm II (NSGA-II), ranking individuals by comparing their objective function values rather than assigning weights to the objectives. However, to enhance efficiency and reduce computational overhead, we deviate from the NSGA-II approach. Rather than categorizing all individuals into distinct levels, we focus on identifying and updating Pareto optimal solutions classified as level 1 dominance (signifying a dominated number of 0) in each iteration. Individuals with a dominance level of 1 are those who are not dominated by any other individual. This means that the solutions represented by these individuals are not worse than any other solutions in all objectives and are strictly better in at least one objective. The remaining Pareto solutions are stored in a set designated for level 2 dominance. **Table 4** shows the pseudocode for fast non-dominated sorting.

Table 4. Basic pseudocode for fast non-dominated sorting

```
Compare the values of the two objective functions corresponding to each individual, and calculate the number
of dominated individuals in the population.
    For each individual in the population
        If the number of dominated equals 0
            The individual enters a set with level 1 dominance.
        else there exists a dominated number
            The individual enters a set with level 2 dominance.
        End if
    End for
All individuals in the population are in order.
```

*4.2.5. Algorithm flow*

The specific steps of the algorithm are shown in **Figure 4**.

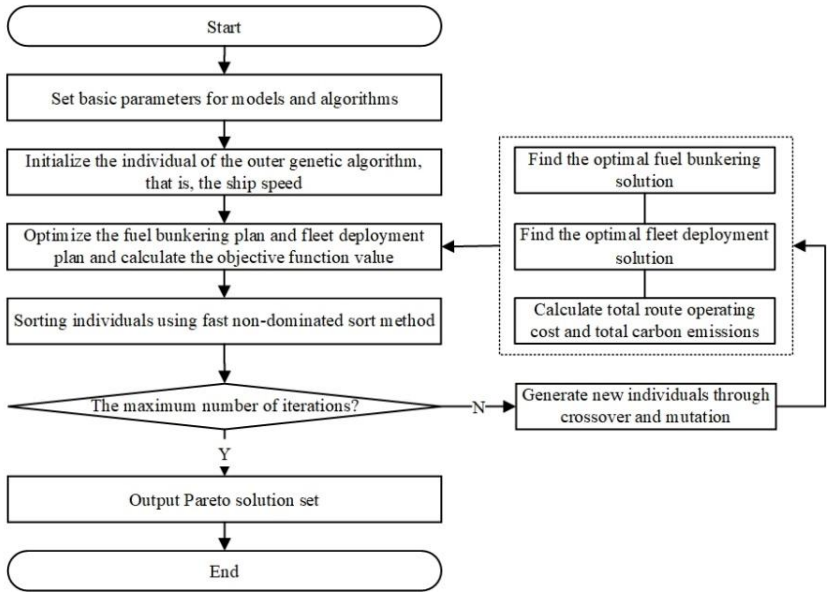


Figure 4. Algorithm flow of MOGA

***Step 1: Parameter setting***

Define model parameters of ships, fuels, and routes. Set the basic parameters of the inner and outer GAs.

***Step 2: Initialization***

Initialize the population, wherein each individual (i.e., chromosome) represents the speed in each leg. For each individual, carry out an exhaustive evaluation of all routes and ship types. Determine the suitability of ship types for a particular route based on the fuel that can be bunkered at the departure port. After making speed decisions, optimize the fuel bunkering and fleet deployment plans for various ship types, resulting in the return of two objective function values. **Table 5** presents the pseudocode for the initialization process.

***Step 2.1: Fuel bunkering decision***

Based on the speed determined for each leg, call the GA to initialize the fuel bunkering variable as an individual under constraints (6)-(8), (13)-(14), and (16)-(17). Subsequently, compute objective functions (1)-(2), and sort the individuals by fast non-dominated sorting. Throughout the iterative process, perform crossover and mutation, and judge whether the solution satisfies constraints (6)-(8), (13)-(14) and (16)-(17). Next, calculate objective functions (1)-(2), compare individuals, and update the population. After that, use fast non-dominated sorting to sort the individuals of the population. Repeat this procedure until reaching the maximum number of iterations.

***Step 2.2: Fleet deployment decision***

Based on the determined ship speed and fuel bunkering, call the GA again to decide on fleet deployment under constraints (4)-(5), (15), and (18). The process mirrors the approach employed in ***Step 2.1***.

***Step 3: Fast non-dominated sorting***

Sort the initial individuals by fast non-dominated sorting.

***Step 4: Iteration***

Perform crossover and mutation on the sorted individuals to generate new individuals, calculate the value of the objective functions, compare individuals, and update the population. Next, sort the individuals in the updated population again by fast non-dominated sorting.

***Step 5: Termination***

When the outer algorithm reaches the maximum number of iterations, terminate its operation to output the Pareto solution set.

Table 5. Pseudocode for the MOGA initialization process

| |
|---|
| For each speed individual $s$ |

Calculate $T_{ris}$, $\beta^{A}_{rivkf}$ and $\beta^{F}_{rivkff'}$ according to the speed determined for each leg $w_{ris}$ under constraints (6)-(8), (13)-(14), and (16)-(17)
For each $r$
For each $v$
If the departure port can bunker fossil fuels for DF ships and alternative fuels for FC ships
Call the GA to calculate $\alpha^{A}_{rivkf}$ and $\alpha^{F}_{rivkff'}$ according to constraints (9)-(10) and (13)-(14)
Calculate $\pi^{A}_{rivkf}$ and $\pi^{F}_{rivkff'}$, and record route and ship data
Else
Conclude that this type of ship is not suitable for this route, and record that the route and ship data are empty.
End if
End for
End for
For each $r$
Calculate the total volume of freight transported and total time of each route
Call the GA to calculate $x_{rvkf}$ under constraints (4)-(5), (15) and (18)
Record route and ship data
End for
Calculate and record the value of objective functions (1)-(2).
End for

Based on the obtained Pareto solution set and the fuzzy decision-making method discussed in Section 4.1, we derive the optimal solutions for different decision makers economic and environmental preferences in terms of heterogeneous fleet deployment, speed determination, and fuel bunkering. It is important to note that in the case of the customized MOGA, the ideal and farthest points for each objective are set to the minimum and maximum values of those two objectives within the Pareto solution set.

## 5. Computational study

After linearization of the BO-MINLP constructed for GLSP, we solve the epsilon constraint method using the CPLEX 20.1.0 solver, which employs the Branch & Cut algorithm. The designed MOGA is implemented through MATLAB R2022a. The computational experiments were conducted on a computer running Windows 11 (64-bit) with a 12th Gen Intel(R) Core TM i7-12700H processor clocked at 2.30 GHz.

### *5.1. Data information*

In this study, we select the company SITC, headquartered in Hong Kong, as our research subject. SITC is a leading liner company in the Asian region, primarily operating on intra-Asian short sea routes.

#### *5.1.1. Routes and port information*

Regarding the route network, we have chosen five routes operated by SITC in Northeast Asia and Southeast Asia, as illustrated in **Figure 5**. Information about the ports, legs (distances), and port calling times on these routes can be found in **Appendix Table A1**. **Table 6** provides the types of fuel that can be bunkered, fuel prices, the volume of freight transported, and other relevant information at each port along these routes. Regarding fuel bunkering prices, we select point observations as an example to illustrate the model. However, it is essential to note that fuel prices can naturally fluctuate over time. Furthermore, the fuel prices for VLSFO and MGO are sourced from August and September 2023 (Marine online, 2023; CNSS, 2023; Ship & Bunker, 2023). The prices for other alternative fuels are estimated based on references and randomly selected within their respective upper and lower price limits. The price of LNG is based on the studies by You et al. (2023), DNV GL (2020), and Lagemann et al. (2022). Methanol prices are derived from Zhao et al. (2023). The price of ammonia is sourced from the research by Yang and Lam (2023) and Wang et al. (2023). Hydrogen prices are taken from Lindstad et al. (2023). For each port, the volume of freight transported was estimated by the authors within a specified range based on the average weekly volume of each route in 2022 (SITC, 2023).

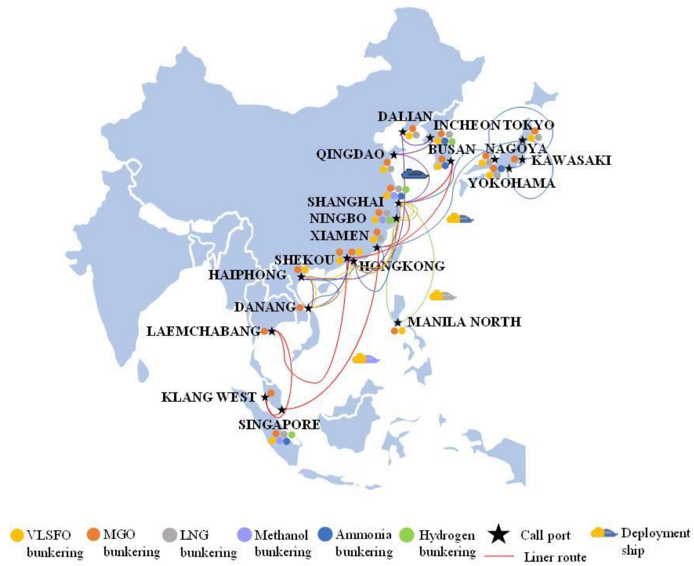


Figure 5. Routes network operated by SITC

Table 6. Port fuel prices and the volume of freight transported on various routes

**FEM2**

| Port | VLSFO (USD/T) | MGO (USD/T) | LNG (USD/T) | Methanol(USD/T) | Ammonia(USD/T) | Hydrogen(USD/T) | The volume of freight transported (TEU) |
|---|---|---|---|---|---|---|---|
| BUSAN | 593 | 723 | - | - | 772 | - | 137 |
| SHANGHAI | 588 | 980 | 847 | 558 | 618 | 4731 | 653 |
| XIAMEN | 555 | 739 | 781 | - | - | - | 271 |
| SINGAPORE | 567 | 908 | 821 | 562 | 562 | 3826 | 161 |
| KLANG WEST | - | 900 | - | - | - | - | 294 |
| LAEMCHABANG | - | 807 | - | - | - | - | 701 |
| SHEKOU | 565 | 829 | - | - | - | - | 454 |

**CJV5**

| Port | VLSFO (USD/T) | MGO (USD/T) | LNG (USD/T) | Methanol(USD/T) | Ammonia(USD/T) | Hydrogen(USD/T) | The volume of freight transported (TEU) |
|---|---|---|---|---|---|---|---|
| NINGBO | 524 | 826 | 719 | 486 | - | 4103 | 803 |
| SHANGHAI | 588 | 980 | 847 | 558 | 618 | 4731 | 524 |
| HONGKONG | 583 | 957 | - | - | - | - | 856 |
| HAIPHONG | 728 | 672 | - | - | - | - | 852 |
| DANANG | - | 812 | - | - | - | - | 446 |
| HONGKONG | 583 | 957 | - | - | - | - | 306 |

**CKV**

| Port | VLSFO (USD/T) | MGO (USD/T) | LNG (USD/T) | Methanol(USD/T) | Ammonia(USD/T) | Hydrogen(USD/T) | The volume of freight |
|---|---|---|---|---|---|---|---|

| | | | | | | | transported (TEU) |
|---|---|---|---|---|---|---|---|
| DALIAN | 550 | 672 | 904 | - | - | - | 330 |
| INCHON | 569 | 689 | 916 | - | 729 | 3038 | 542 |
| QING DAO | 562 | 765 | 759 | - | - | - | 313 |
| SHANG HAI | 588 | 980 | 847 | 558 | 618 | 4731 | 263 |
| HAIPHONG | 728 | 672 | - | - | - | - | 364 |
| DANANG | - | 812 | - | - | - | - | 579 |
| SHEKOU | 565 | 829 | - | - | - | - | 241 |

**CJV6**

| Port | VLSFO (USD/T) | MGO (USD/T) | LNG (USD/T) | Methanol(USD/T) | Ammonia(USD/T) | Hydrogen(USD/T) | The volume of freight transported (TEU) |
|---|---|---|---|---|---|---|---|
| SHANGHAI | 588 | 980 | 847 | 558 | 618 | 4731 | 647 |
| HONGKONG | 583 | 957 | - | - | - | - | 653 |
| HAIPHONG | 728 | 672 | - | - | - | - | 652 |
| DANANG | - | 812 | - | - | - | - | 543 |
| SHEKOU | 565 | 829 | - | - | - | - | 869 |
| XIAMEN | 555 | 739 | 781 | - | - | - | 519 |
| TOKYO | 681 | 740 | 823 | - | - | 4852 | 690 |
| YOKOHAMA | 590 | 962 | 832 | - | 506 | - | 384 |
| KAWASAKI | - | 696 | - | - | - | - | 279 |
| NAGOYA | 575 | 685 | 895 | - | - | - | 580 |

**CPS**

| Port | VLSFO (USD/T) | MGO (USD/T) | LNG (USD/T) | Methanol(USD/T) | Ammonia(USD/T) | Hydrogen(USD/T) | The volume of freight transported (TEU) |
|---|---|---|---|---|---|---|---|
| SHANGHAI | 588 | 980 | 847 | 558 | 618 | 4731 | 623 |
| NINGBO | 524 | 826 | 719 | 486 | - | 4103 | 598 |
| MANILANORTH | 1560 | 867 | - | - | - | - | 422 |

*5.1.2. Ship and fuel information*

SITC's fleet consists of container ships with cargo hold capacities ranging from 787 to 2,741 TEU, with 1,800 TEU and 2,600 TEU ships being the primary types. In this case, the heterogeneous fleet comprises both 1,800 TEU and 2,600 TEU container ships. Information regarding the cargo hold capacity, power system, alternative fuel, and storage tank capacity for these ships can be found in **Table 7**. The storage tank capacity of each ship's fuel was estimated based on studies by Wu et al. (2022a), Pekic (2022), and Tan et al. (2020), considering the density of different fuels. The maximum available volumes of 1,800 TEU and 2,600 TEU ships are 10 and 5 respectively, with a speed range of 13-20 KN. Details about the ship's design speed, reference power, and fuel combustion efficiency, as well as information about fuel emission factors, low calorific value, and density can be found in **Appendix Tables A2-A3**. In addition, the fixed costs of deploying different types of container ships when completing an entire route, including capital costs, crew wages, insurance premiums, and other factors, are calculated based on the ship investment costs as study by Zou and Yang (2023), as shown in **Appendix Table A4**.

Table 7. Ship information on different ship types

| Cargo hold capacity (TEU) | Power system | Fuel storage tank capacity (T) | | | | | |
|---|---|---|---|---|---|---|---|
| | | VLSFO | MGO | LNG | Methanol | Ammonia | Hydrogen |
| 1,800 | VLSFO+MGO DF | 1,280 | 1,142 | - | - | - | - |

| | | | | | | | |
|---|---|---|---|---|---|---|---|
| | VLSFO+LNG DF | 1,280 | - | 615 | - | - | - |
| | VLSFO+ Methanol DF | 1,280 | - | - | 1,083 | - | - |
| | VLSFO+ Ammonia DF | 1,280 | - | - | - | 834 | - |
| | VLSFO+ Hydrogen DF | 1280 | - | - | - | - | 97 |
| | Methanol FC | - | - | - | 1,083 | - | - |
| | Ammonia FC | - | - | - | - | 834 | - |
| | Hydrogen FC | - | - | - | - | - | 97 |
| 2,600 | VLSFO+MGO DF | 1,848 | 1649 | - | - | - | - |
| | VLSFO+LNG DF | 1,848 | - | 889 | - | - | - |
| | VLSFO+ Methanol DF | 1,848 | - | - | 1,564 | - | - |
| | VLSFO+ Ammonia DF | 1,848 | - | - | - | 1205 | - |
| | VLSFO+ Hydrogen DF | 1,848 | - | - | - | - | 140 |
| | Methanol FC | - | - | - | 1,564 | - | - |
| | Ammonia FC | - | - | - | - | 1205 | - |
| | Hydrogen FC | - | - | - | - | - | 140 |

**Notes:**

a. Compilation by authors based on reference data from Pekic (2022).

b. Hydrogen is stored in liquid form (at -253° C).

*5.2. Calculated results*

*5.2.1. Solution method test*

We applied the epsilon constraint method and MOGA to test the proposed model on the five routes actually operated by SITC, generating 15 instances based on the number of liner service routes considered. Each instance varied in the number of legs. The population size for MOGA was 50, with maximum iterations of 100 and 20 for the outer and inner layers, respectively. The crossover probability was 0.9, and the mutation probability was 0.9. The results obtained by both methods are presented in **Table 8**, where "-" indicates unresolved cases or memory overflow within a 28000s time limit for the epsilon constraint method, and [Number, Number] shows the lower and upper bounds of objectives in the Pareto solution set.

**Table 8** reveals that the epsilon constraint method is capable of solving problems for small-scale single routes or two-route combinations. However, as the linearization of the original problem required discretization based on cargo hold capacity types. Matching each cargo hold capacity, power system, and alternative fuel needed 120 iterations. As route combinations expanded, solving with CPLEX became increasingly challenging, thus the epsilon constraint method provided solutions for only 6 instances. To contrast with the proposed MOGA method, we applied the epsilon constraint method to decompose instances into single routes for solution.

Compared to the non-decomposed epsilon constraint method, the proposed MOGA can solve all instances, including large-scale ones. In contrast with the epsilon constraint method that decomposes routes, although both methods can simultaneously obtain solutions, MOGA slightly lags in precision for the lower objective bounds but has an advantage for the upper bounds. This difference is due to the initial solution setup in MOGA. While ensuring feasibility, it results in higher minimum total operating costs and carbon emissions than the epsilon constraint method. Additionally, it can be observed that due to differences in solution approaches, the epsilon constraint method prioritizes low-carbon and zero-carbon objectives, while MOGA's solutions are more diversified.

Table 8. Test results of epsilon constraint method and MOGA on 15 instances

| Instance | Routes (Number | Epsilon constraint (all routes) | Epsilon constraint (single routes) | MOGA |
|---|---|---|---|---|

| | of Ports of Call) | Total operating cost ($10^6$ USD) | Total carbon emissions ($10^3$ T) | CPU time (sec) | Total operating cost ($10^6$ USD) | Total carbon emissions ($10^3$ T) | CPU time (sec) | Total operating cost ($10^6$ USD) | Total carbon emissions ($10^3$ T) | CPU time (sec) |
|---|---|---|---|---|---|---|---|---|---|---|
| 1 | FEM2(7) | [1.14,2.13] | [0.00,3.67] | 4557 | [1.14,2.13] | [0.00,3.67] | 4557 | [1.71,2.10] | [1.31,3.37] | 2579 |
| 2 | CJV5(6) | [0.28,0.59] | [0.00,0.83] | 1276 | [0.28,0.59] | [0.00,0.83] | 1276 | [0.40,0.59] | [0.45,0.87] | 2879 |
| 3 | CKV(7) | [0.58,1.02] | [0.00,2.05] | 4884 | [0.58,1.02] | [0.00,2.05] | 4884 | [0.93,1.09] | [1.51,1.80] | 3316 |
| 4 | CJV6(10) | [0.68,1.30] | [0.00,2.06] | 1653 | [0.68,1.30] | [0.00,2.06] | 1653 | [1.26,1.50] | [0.00,1.50] | 4002 |
| 5 | CPS(3) | [0.21,0.44] | [0.00,0.70] | 1414 | [0.21,0.44] | [0.00,0.70] | 1414 | [0.31,0.38] | [0.32,0.70] | 1756 |
| 6 | FEM2(7), CPS(3) | - | - | 28000 | [1.35,2.57] | [0.00,4.37] | 5971 | [2.26,2.53] | [2.16,3.39] | 4266 |
| 7 | CJV5(6), CPS(3) | [0.49,1.02] | [0.00,1.53] | 7886 | [0.49,1.03] | [0.00,1.53] | 2690 | [0.84,0.99] | [0.84,1.39] | 4661 |
| 8 | CKV(7), CJV6(10) | - | - | 28000 | [1.26,2.32] | [0.00,4.11] | 6537 | [2.32,2.84] | [2.33,3.81] | 5743 |
| 9 | FEM2(7), CJV5(6), CKV(7) | - | - | 28000 | [2.00,3.74] | [0.00,6.55] | 10717 | [3.44,3.72] | [4.63,6.49] | 7166 |
| 10 | FEM2(7), CJV5(6), CPS(3) | - | - | 28000 | [1.63,3.16] | [0.00,5.20] | 7247 | [2.70,3.15] | [3.31,4.53] | 7184 |
| 11 | FEM2(7), CKV(7), CJV6(10) | - | - | 28000 | [2.40,4.45] | [0.00,7.78] | 10855 | [4.22,4.69] | [5.10,6.72] | 7892 |
| 12 | FEM2(7), CJV5(6), CKV(7), CJV6(10), | - | - | 28000 | [2.68,5.04] | [0.00,8.61] | 12370 | [5.06,5.87] | [6.07,8.27] | 11163 |
| 13 | FEM2(7), CKV(7), CJV6(10), CPS(3) | - | - | 28000 | [2.61,4.89] | [0.00,8.48] | 12508 | [4.96,5.56] | [5.20,7.70] | 9823 |
| 14 | CJV5(6), CKV(7), CJV6(10), CPS(3) | - | - | 28000 | [1.75,3.35] | [0.00,5.64] | 9227 | [3.26,3.80] | [3.69,5.83] | 10287 |
| 15 | FEM2(7), CJV5(6), CKV(7), CJV6(10), CPS(3) | - | - | 28000 | [2.89,5.48] | [0.00,9.31] | 13784 | [5.39,5.95] | [6.30,8.35] | 12858 |

*5.2.2. Planning decision analysis*

Subsequently, we analyze the planning decisions for a large-scale instance that includes five routes (33 legs), which corresponds to SITC's actual operation. The results show the Pareto solution sets, Pareto frontiers, and the corresponding fleet deployment decisions, as depicted in **Figure 6**.

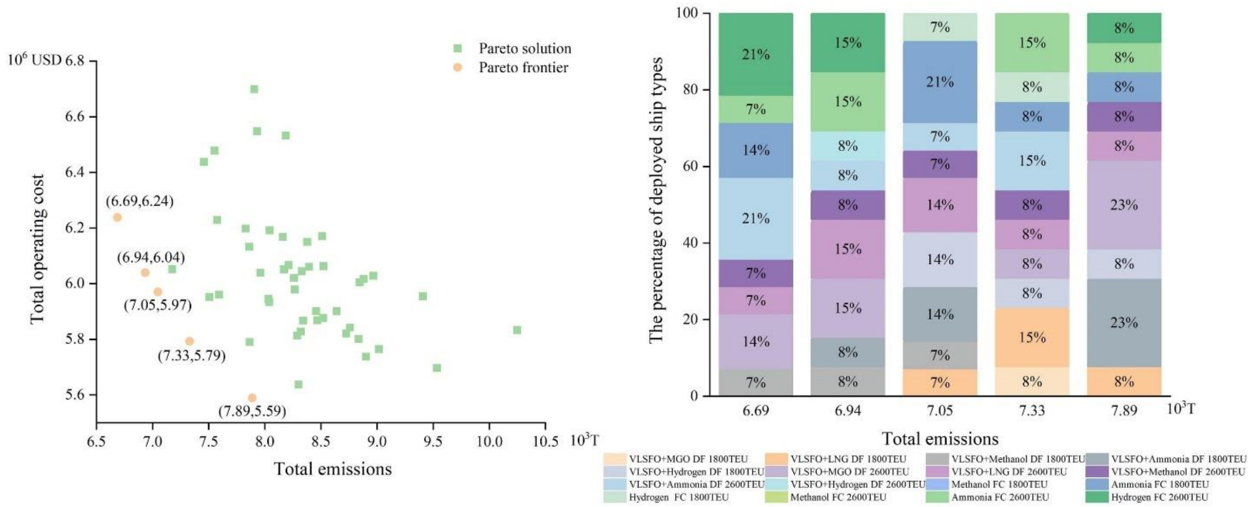


Figure 6. Pareto solution sets, Pareto frontiers, and corresponding fleet deployment decisions obtained by MOGA

**Notes:**

a. The Pareto solution set for each run presents 50 (population size) solutions;

b. The fleet deployment decisions corresponding to the Pareto frontiers are presented based on the corresponding total carbon emissions.

Firstly, it can be learned from the distribution of Pareto frontiers that there's a clear conflict between minimizing operating costs and reducing $CO_2$ emissions: pursuing sustainability often comes at a significant expense. Liner companies can achieve a balance between these objectives based on their preferences, ultimately determining the optimal solution. If carbon emissions are not a significant concern (i.e., $\omega 1=1,\ \omega 2=0$), the solution with the lowest total operating cost is 5.59 million USD, with total carbon emissions of 7,888.93 T. Meanwhile, if cost control is not a primary consideration (i.e., $\omega 1=0,\ \omega 2=1$), the solution with the lowest total carbon emissions results in 6,686.92 T but with a total operating cost of 6.69 million USD. To achieve a balance between cost efficiency and environmental responsibility and contribute to global sustainability, liner companies might prefer a strategy where $\omega 1=\omega 2=0.5$. This approach results in a solution with total carbon emissions of 7,329.94 T and a total operating cost of 5.79 million USD.

Secondly, we can observe how the ship deployment structure changes with different total carbon emissions. In general, DF ships play an important role in the low-carbon operations of liner companies. DF ships using LNG and ammonia are among the most frequently chosen ship types, followed by those using methanol, MGO, and hydrogen. When decision-makers prioritize lower $CO_2$ emissions, FC ships, especially ammonia and hydrogen FC ships, need to be supplemented. This is because the $CO_2$ emissions of DF ships using LNG and ammonia, although lower than those using MGO, are significantly higher than those of FC ships using ammonia and hydrogen due to the use of fossil fuels (see **Table A3** for relevant emission factors). Additionally, irrespective of the chosen power system and alternative fuel, 2,600 TEU ships demonstrate a greater advantage in reducing costs than 1,800 TEU ships. It appears that deploying larger ships on the route network is suitable for liner companies pursuing low-carbon and zero-carbon objectives (Pasha et al., 2021), given some level of economies of scale in energy consumption.

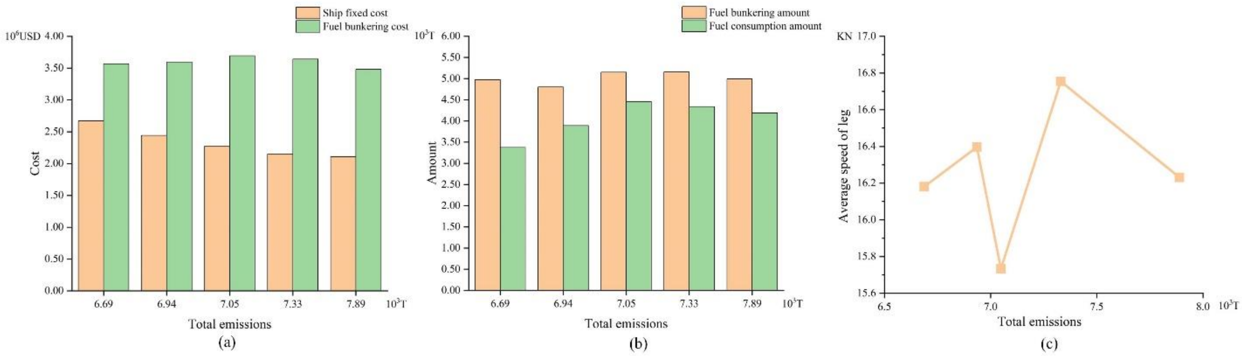


Figure 7. Additional decision results obtained by MOGA

**Notes:**

a. Relationship between fixed ship cost, variable fuel bunkering cost, and total carbon emissions;
b. Relationship between fuel bunkering, fuel consumption, and total carbon emissions;
c. Relationship between average speed for all legs and total carbon emissions.

**Figure 7(a)** illustrates the evolving relationship between fixed ship cost, variable fuel bunkering cost, and total carbon emissions. Notably, as total carbon emissions decrease, fixed ship costs exhibit an upward trend, while variable fuel bunkering costs show fluctuations. Moreover, in general, variable fuel bunkering cost is typically about twice the amount of fixed ship cost, making up a significant portion (57%-62%) of the total operating cost, in line with the observations made by Notteboom and Vernimmen (2019), Ronen (2011) and Wang et al. (2018).

**Figure 7(b)** displays the relationship between fuel bunkering volume, fuel consumption volume, and total carbon emissions. In tandem with the reduction in total carbon emissions, the higher variable fuel bunkering cost signifies an increase in the fuel bunkering volume. As a rule, to ensure that container ships can fulfill their services on their designated routes, the fuel bunkering volume consistently surpasses the fuel consumption. Among all solutions, the maximum difference between these two values stands at 1,600 T, approximately 30% of the fuel bunkering volume. The fluctuations observed in Figures 7(a) and 7(b) mainly come from fleet deployment decisions influenced by variations in ship structure, reflecting the optimization results of fuel management under various real-world factors.

**Figure 7(c)** shows the changing relationship between the average speed across all legs and total carbon emissions. The average speed across all legs ranges from 15.7 to 16.8 KN, demonstrating that a uniform minimum speed approach is not applied. Furthermore, there was no clear correlation between the average speed of all legs and total carbon emissions. Consequently, for a green heterogeneous fleet, speed determination is an auxiliary decision, which can be closely coordinated with fleet deployment and fuel bunkering. The flexible coordination enables carbon reduction in liner shipping.

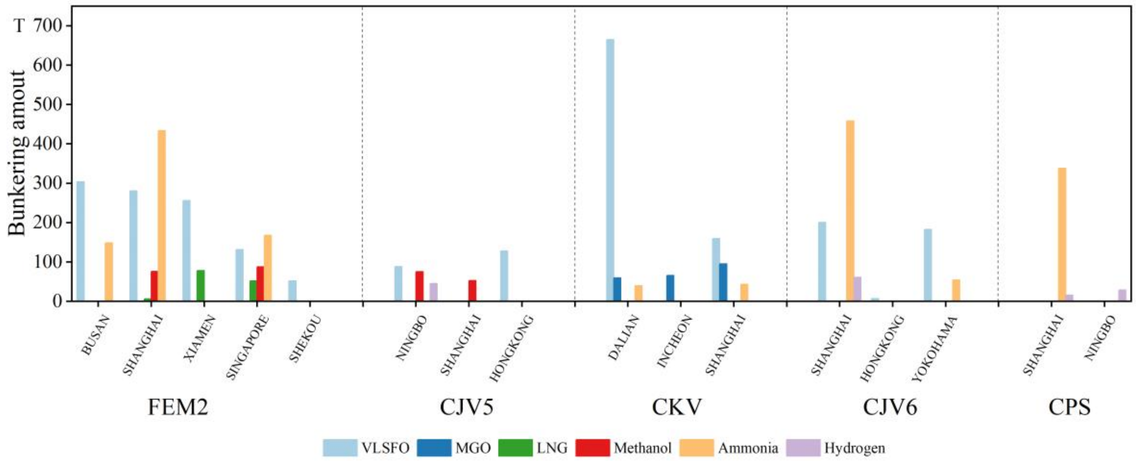


(a) When the total cost is 6.24 million USD and the total emissions are 6,686.92 T

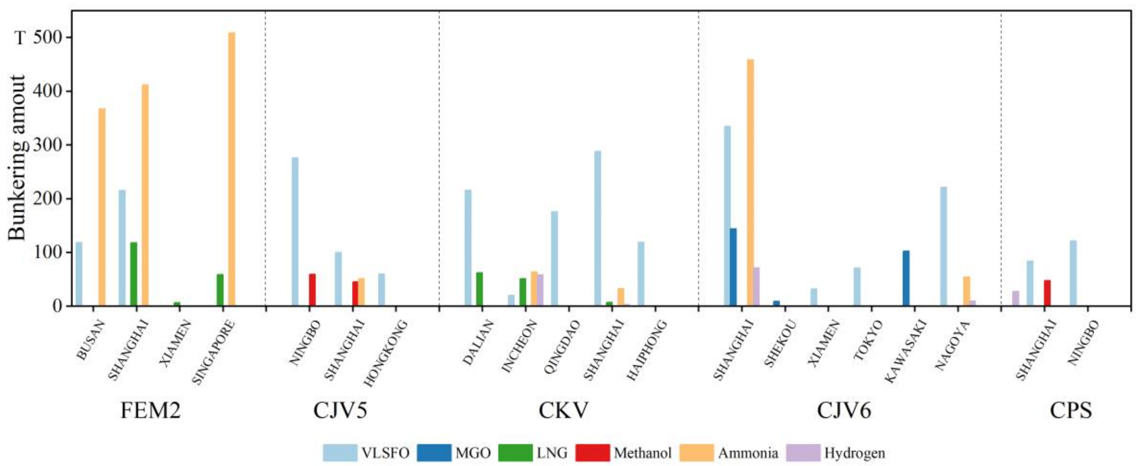


(b) When the total cost is 6.04 million USD and the total emissions are 6,935.08 T

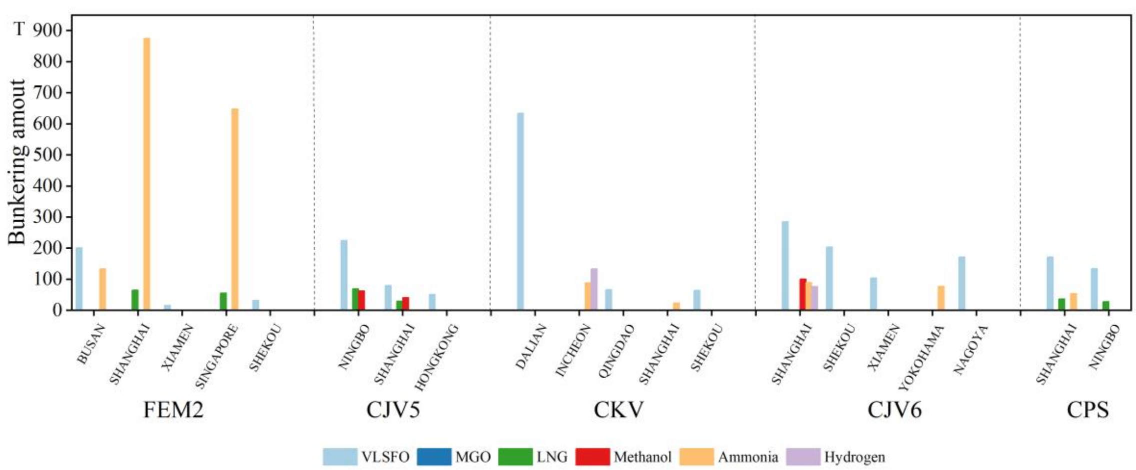


(c) When the total cost is 5.97 million USD and the total emissions are 7,048.17 T

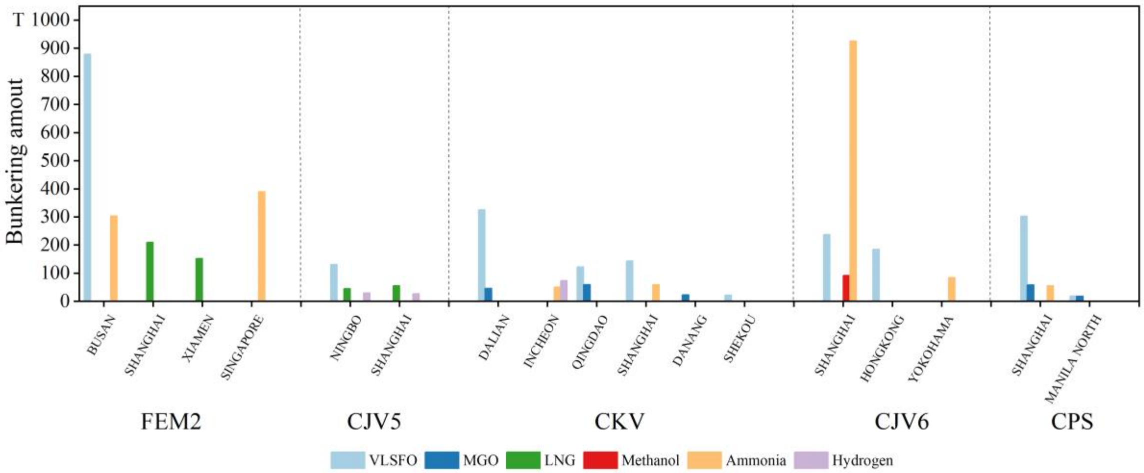


(d) When the total cost is 5.79 million USD and the total emissions are 7,329.94 T

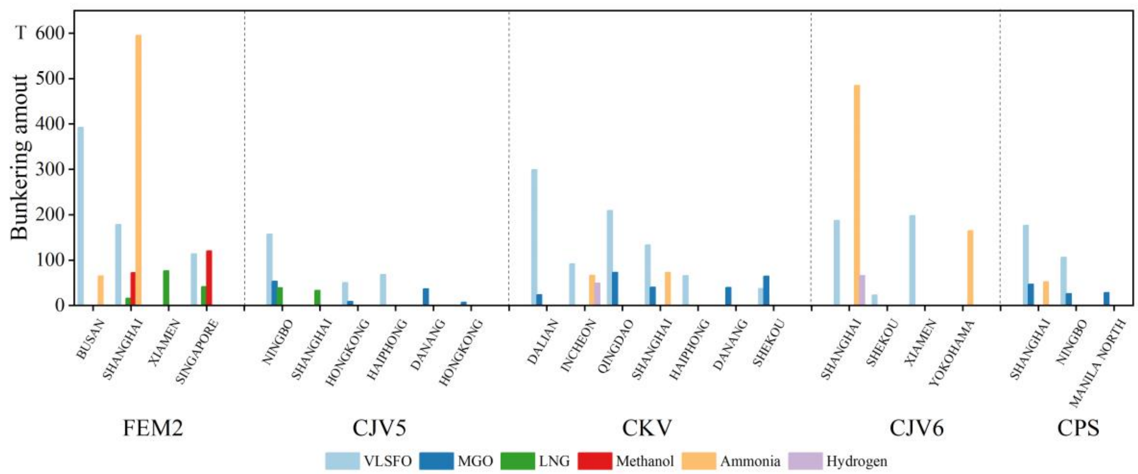


(e) When the total cost is 5.59 million USD and the total emissions are 7,888.93 T

Figure 8 Decisions regarding the selection of fuel bunkering ports and bunkering amount for each route corresponding to different Pareto frontiers

**Notes:**

Only the ports with bunkering decisions on each route are shown in the figure.

**Figure 8** presents the decisions regarding the selection of fuel bunkering ports and bunkering amount for each route corresponding to different Pareto frontiers. In fact, the selection of fuel bunkering ports and the decisions regarding bunkering amount are closely tied to fleet deployment and speed determination decisions. Additionally, these decisions depend on fuel consumption between legs, fuel inventory, and fuel prices at different ports. According to **Table 5**, ports with lower fuel prices are prioritized, as seen in FEM2 for VLSFO in **Figure 8(a)**. When fuel inventory is insufficient for the entire voyage, small amounts of high-priced fuel are bunkered, as shown for CJV6 in **Figure 8(a)**. Constraints in bunkering ports can also lead to high-priced bunkering, such as for hydrogen in CJV5 in **Figure 8(d)**. If fuel inventory is sufficient for the entire voyage, no additional fuel is bunkered, as seen in **Figure 8** where certain fuels are bunkered at only one port.

## 6. Conclusions

Under the ambitious carbon reduction targets set by the IMO, liner companies are poised to undergo transformative changes in both technology and operation. This paper defines and explores the GLSP problem, which integrates heterogeneous fleet deployment, speed determination, and fuel bunkering. This problem differs significantly from the previous approaches that focused on homogeneous fleet deployment using DF technology on single routes (Wu et al., 2022a; Tan et al., 2020). We propose a BO-MINLP model considering the characteristics of the heterogeneous fleet (e.g., cargo hold capacity, power system, and alternative fuel), as well as factors like inherent service frequency, the volume of freight transported in liner shipping, various bunkering ports, and alternative fuel bunkering prices. Moreover, we develop an epsilon constraint-based approach and a heuristic-based MOGA. The effectiveness of these model and methods was demonstrated through a case study involving container vessels of different sizes operated by SITC on intra-Asian short sea routes. While our customized MOGA may not be as precise as the epsilon constraint-based method for small-scale problems, it demonstrates superior performance in diversifying the Pareto front and solving large-scale instances.

The results of the planning decision analysis reveal a significant conflict between the two objectives of minimizing total operating cost and reducing total carbon emissions, requiring decision-makers to strike a balance. In terms of fleet deployment, DF ships, especially those using LNG and ammonia, play a pivotal role, although FC ships, especially those powered by ammonia and hydrogen, offer substantial carbon reduction potential. Furthermore, ships with large cargo hold capacity maintain a cost advantage. Regarding speed determination and fuel bunkering, liner companies striving for low-carbon operations are challenged to deploy more alternative fuel ships. The ensuring increase of fuel bunkering volume and fuel consumption would push up the total operating cost. Speed determination is an auxiliary decision, and solutions at the given fuel prices do not necessarily minimize speed. Furthermore, limitations on bunkering ports can significantly impact bunkering decisions, potentially forcing companies to overlook high fuel prices to complete their voyages.

In summary, the decision-making of fleet deployment, speed determination, and fuel bunkering for a green heterogeneous fleet requires comprehensive optimization under various real-world factors. Obviously, the findings are intrinsic to the used input data on ship operations (routes, ship size, fuel) and related costs and prices, implying the results cannot be generalized to other (green) liner shipping settings. In this regard, the empirical application of SITC was primarily included for illustrative purposes on how the BO-MINLP model can be applied to solve GSLP in real-world cases.

Future research on GLSP should consider the uncertainty in the shipping market, such as random variations in fuel bunkering prices at different ports and fluctuations in the volume of freight transported. In addition, it is possible to design improved fuel bunkering strategies to enhance algorithm precision. Furthermore, extensive research has been conducted on heuristic algorithms and their hybrids as tools for solving single-objective or multi-objective combinatorial optimization problems (Dokeroglu et al., 2019; Singh et al., 2022). Metaheuristic algorithms, which are higher-level heuristic methods, have been proposed to address a wide range of optimization problems. Hyper-heuristics aim to enhance the level of generality by focusing on selecting the appropriate (meta)heuristic under varying conditions (Singh and Pillay, 2022). These advanced optimization algorithms have been successfully applied in various fields, such as scheduling, transportation, medicine, and reinforcement learning, demonstrating their effectiveness (Dulebenets, 2021; Dulebenets, 2023; Chen and Tan, 2023). Future research will explore the application of advanced optimization algorithms to address the decision problems presented in this study and compare them with the methods proposed herein.

## CRediT authorship contribution statement

**Yuzhe Zhao**: Conceptualization, Methodology, Writing - Review & Editing, Funding acquisition. **Zhongxiu Peng**: Software, Data Curation, Writing - Original Draft, Visualization. **Jingmiao Zhou**: Formal analysis, Writing - Review & Editing, Project administration. **Theo Notteboom:** Review & Editing, Resources, Supervision. **Yiji Ma:** Investigation, Validation.

## Declaration of competing interest

The authors declare that they have no known competing financial interests or personal relationships that could have appeared to influence the work reported in this paper.

## Acknowledgements

The work was supported in part by National Natural Science Foundation of China [grant numbers 72072017, 71902016, 71831002]; Foundation for Humanities and Social Sciences of Ministry of Education of China [grant number 23YJCZH329]; Natural Science Foundation of Liaoning Province of China [grant number 2022-MS-162, 2023-MS-275]; Fundamental Research Funds for the Central Universities [grant number 3132023702].

**References**

ABS, 2019. Setting the course to low carbon shipping - 2030 OUTLOOK | 2050 VISION. https://absinfo.eagle.org/acton/attachment/16130/f-982b1623-4d26-4b04-91c5-25453a6e2fba/1/-/-/-/-/low-carbon-shipping-outlook.pdf (accessed 6 July 2023).

Azane Fuel Solutions, 2023. Building an ammonia fuel bunkering network. https://www.azanefs.com/ (accessed 17 September 2023).

Basnet, C., Weintraub, A., 2009. A genetic algorithm for a bicriteria supplier selection problem. *International Transactions in Operational Research* 16, 173-187. https://doi.org/10.1111/j.1475-3995.2009.00680.x

Bui, K.Q., Perera, L.P., Emblemsvåg, J., 2022. Life-cycle cost analysis of an innovative marine dual-fuel engine under uncertainties. *Journal of Cleaner Production* 380, 134847. https://doi.org/10.1016/j.jclepro.2022.134847

Cariou, P., Parola, F., Notteboom, T., 2019. Towards low carbon global supply chains: A multi-trade analysis of CO2 emission reductions in container shipping. *International Journal of Production Economics*, 208, 17-28. https://doi.org/10.1016/j.ijpe.2018.11.016

CCS, 2021. Low carbon development outlook for shipping 2021. https://www.ccs.org.cn/ccswz/articleDetail?id=202111050991394944.

CCS, 2023. Low carbon development outlook for shipping 2023. https://www.ccs.org.cn/ccswz/articleDetail?id=202312081257422748.

Christiansen, M., Fagerholt, K., Nygreen, B., Ronen, D., 2013. Ship routing and scheduling in the new millennium. *European Journal of Operational Research* 228, 467-483. https://doi.org/10.1016/j.ejor.2012.12.002

Chen, M., Tan, Y., 2023. SF-FWA: A Self-Adaptive Fast Fireworks Algorithm for effective large-scale optimization. *Swarm and Evolutionary Computation* 80, 101314. https://doi.org/10.1016/j.swevo.2023.101314

Clarksons, 2023a. Port &. Infrastructure intelligence monthly. https://www.clarksons.net.cn/api/download/SIN/download/e6eb64b3-bb77-467f-9bb0-7de47f8a3201?downloadInline=true (accessed 24 September 2023).

Clarksons, 2023b. Seaborne trade monitor. https://www.clarksons.net.cn/api/download/SIN/download/4476e445-728f-4c4a-a556-71d2627fee96?downloadInline=true (accessed 24 September 2023).

Clarksons, 2023c. World fleet monitor. https://www.clarksons.net.cn/api/download/SIN/download/aafd031b-1b54-40ab-b4b9-b6d7e4f3b72b?downloadInline=true (accessed 24 September 2023).

CNSS, 2023. Port fuel price. https://www.cnss.com.cn/html/gkryjg/20230923/350900.html (accessed 22 September 2023).

De, A., Kundu, T., Sheu, J.-B., Choi, T.-M., 2023. Sailing smoothly under Sulphur fuel regulations: The shipping liner's bunkering problem. *Transportation Research Part D: Transport and Environment* 121, 103838. https://doi.org/10.1016/j.trd.2023.103838

DNV, 2023. Maritime forecast to 2050 – Energy transition outlook 2023. https://www.dnv.com/maritime/publications/maritime-forecast-2023/index.html(accessed 21 September 2022).

DNV, 2024. Alternative fuels insight. https://afi.dnv.com/statistics/16486173-4f14-4cc5-b9f6-f2f4b4c47a15 (accessed 18 June 2024).

DNV GL, 2020. Maritime forecast to 2050 – Energy transition outlook 2020. https://sustainableworldports.org/wp-content/uploads/DNV-GL_2019_Maritime-forecast-to-2050-Energy-transition-Outlook-2019-report.pdf (accessed 10 August 2022).

Dokeroglu, T., Sevinc, E., Kucukyilmaz, T., Cosar, A., 2019. A survey on new generation metaheuristic algorithms. *Computers & Industrial Engineering* 137, 106040. https://doi.org/10.1016/j.cie.2019.106040

Dulebenets, M.A., 2021. An Adaptive Polyploid Memetic Algorithm for scheduling trucks at a cross-docking terminal. *Information Sciences* 565, 390-421. https://doi.org/10.1016/j.ins.2021.02.039

Dulebenets, M.A., 2023. A Diffused Memetic Optimizer for reactive berth allocation and scheduling at marine container terminals in response to disruptions. *Swarm and Evolutionary Computation* 80, 101334. https://doi.org/10.1016/j.swevo.2023.101334

EPRS, 2020. Decarbonising maritime transport: The EU perspective. https://www.europarl.europa.eu/RegData/etudes/BRIE/2020/659296/EPRS_BRI(2020)659296_EN.pdf (accessed 10 August 2022).

Ha, M.H., Park, H. and Seo, Y.J., 2023. Understanding core determinants in LNG bunkering port selection: Policy implications for the maritime industry. *Marine Policy* 152, 105608. https://doi.org/10.1016/j.marpol.2023.105608

Hydrogen Council, 2020. Path to hydrogen competitiveness A cost perspective. https://hydrogencouncil.com/wp-content/uploads/2020/01/Path-to-Hydrogen-Competitiveness_Full-Study-1.pdf (accessed 17 September 2023).

IEA, 2023. Tracking Shipping. https://www.iea.org/energy-system/transport/international-shipping (accessed 17 September 2023)

IMO, 2023. Revised GHG reduction strategy for global shipping adopted. https://www.imo.org/en/MediaCentre/PressBriefings/pages/Revised-GHG-reduction-strategy-for-global-shipping-adopted-.aspx (accessed 17 September 2023).

ITF, 2018. Decarbonising Maritime Transport: Pathways to zero-carbon shipping by 2035. International Transport Forum Policy Papers, No. 47, OECD Publishing, Paris. https://doi.org/10.1787/b1a7632c-en

Korberg, A.D., Brynolf, S., Grahn, M., Skov, I.R., 2021. Techno-economic assessment of advanced fuels and propulsion systems in future fossil-free ships. *Renewable and Sustainable Energy Reviews* 142, 110861. https://doi.org/10.1016/j.rser.2021.110861

Kramel, D., Muri, H., Kim, Y., Lonka, R., Nielsen, J.B., Ringvold, A.L., Bouman, E.A., Steen, S., Strømman, A.H., 2021. Global shipping emissions from a well-to-wake perspective: The MariTEAM model. *Environmental Science & Technology* 55, 15040-15050. https://doi.org/10.1021/acs.est.1c03937

Lagemann, B., Lindstad, E., Fagerholt, K., Rialland, A., Ove Erikstad, S., 2022. Optimal ship lifetime fuel and power system selection. *Transportation Research Part D: Transport and Environment* 102, 103145. https://doi.org/10.2139/ssrn.4367982

Lindstad, E., Lagemann, B., Rialland, A., Gamlem, G.M., Valland, A., 2021. Reduction of maritime GHG emissions and the potential role of E-fuels. *Transportation Research Part D: Transport and Environment* 101, 103075. https://doi.org/10.1016/j.trd.2021.103075

Liu, M., Liu, X., Ch, F., Zhu, M., Zheng, F., 2019. Liner ship bunkering and sailing speed planning with uncertain demand. *Computational & Applied Mathematics* 39, 22. https://doi.org/10.1007/s40314-019-0994-2

Liu, X., Xu, Y., Xu, M., Deng, W., Pan, L., Ng, A.K.Y., 2023. Two-hop biconnected components in the global liner shipping network reveal international trade statuses. *IEEE Transactions on Network Science and Engineering* 10, 1564-1574. https://doi.org/10.1109/tnse.2022.3230740

Ma, W., Hao, S., Ma, D., Wang, D., Jin, S., Qu, F., 2021. Scheduling decision model of liner shipping considering emission control areas regulations. *Applied Ocean Research* 106, 102416. https://doi.org/10.1016/j.apor.2020.102416

MAN, 2021. MAN B&W ME-LGIP dual-fuel engines. https://www.man-es.com/docs/default-source/marine/tools/.pdf?sfvrsn=d28a4219_12 (accessed 6 March 2023).

Marine online, 2023.Oil price inquiry. https://www.marineonline.com/bunkering/newBunkerPrice (accessed 6 July 2023).

Mollaoglu, M., Altay, B.C., Balin, A., 2023. Bibliometric review of route optimization in maritime transportation: Environmental sustainability and operational efficiency. *Transportation Research Record* 2677, 879-890. https://doi.org/10.1177/03611981221150922

Notteboom, T.E., Vernimmen, B., 2009. The effect of high fuel costs on liner service configuration in container shipping. *Journal of Transport Geography* 17, 325-337. https://doi.org/10.1016/j.jtrangeo.2008.05.003

Nunes, P., Moura, A., Santos, J., 2023. Solving the multi-objective bike routing problem by meta-heuristic algorithms. *International Transactions in Operational Research* 30, 717-741. https://doi.org/10.1111/itor.13114

Pasha, J., Dulebenets, M.A., Fathollahi-Fard, A.M., Tian, G., Lau, Y.-y., Singh, P., Liang, B., 2021. An integrated optimization method for tactical-level planning in liner shipping with heterogeneous ship fleet and environmental considerations. *Advanced Engineering Informatics* 48, 101299. https://doi.org/10.1016/j.aei.2021.101299

Pekic, S. Hyundai Samho picks GTT tank design for four LNG-fueled containerships. 2022. Available online: https://www.offshore-energy.biz/hyundai-samho-picks-gtt-tank-design-for-four-lng-fuelled-containerships/ (accessed on 23 September 2023).

Ronen, D., 2011. The effect of oil price on containership speed and fleet size. *Journal of the Operational Research Society* 62, 211-216. https://doi.org/10.1057/jors.2009.169

Sarker, R., Runarsson, T.P. and Newton, C., 2001. A Constrained Multiple Raw Materials Manufacturing Batch Sizing Problem. *International Transactions in Operational Research* 8: 121-138. https://doi.org/10.1111/1475-3995.00254

SEA-LNG, 2022. LNG - Transforming the global shipping industry. https://sea-lng.org/wp-content/uploads/2022/01/LNG-2022_A-view-from-the-bridge_V937.pdf (accessed 17 September 2023).

SITC, 2023. SITC 2022 performance. https://www.sitc.com/upfile/202303/2023031637483281.pdf (accessed 6 March 2023).

Ship & Bunker, 2023. Asia/Pacific bunker prices. https://shipandbunker.com/prices/apac (accessed 6 July 2023).

Solakivi, T., Paimander, A., Ojala, L., 2022. Cost competitiveness of alternative maritime fuels in the new regulatory framework. *Transportation Research Part D: Transport and Environment* 113, 103500. https://doi.org/10.1016/j.trd.2022.103500

Singh, P., Pasha, J., Moses, R., Sobanjo, J., Ozguven, E.E., Dulebenets, M.A., 2022. Development of exact and heuristic optimization methods for safety improvement projects at level crossings under conflicting objectives. *Reliability Engineering & System Safety* 220, 108296. https://doi.org/10.1016/j.ress.2021.108296

Singh, E., Pillay, N., 2022. A study of ant-based pheromone spaces for generation constructive hyper-heuristics. *Swarm and Evolutionary Computation* 72, 101095. https://doi.org/10.1016/j.swevo.2022.101095

Sun, X., Chen, J., Liu, W., 2023. Joint maritime bunker hedging and operational consumption based on CVaR optimization. *Journal of Marine Science and Engineering* 11, 894. https://doi.org/10.3390/jmse11050894

Sürer, M.G., Arat, H.T., 2022. Advancements and current technologies on hydrogen fuel cell applications for marine vehicles. *International Journal of Hydrogen Energy* 47, 19865-19875. https://doi.org/10.1016/j.ijhydene.2021.12.251

Tan, R., Duru, O., Thepsithar, P., 2020. Assessment of relative fuel cost for dual fuel marine engines along major Asian container shipping routes. *Transportation Research Part E-Logistics and Transportation Review* 140, 102004. https://doi.org/10.1016/j.tre.2020.102004

The Royal Society, 2020. Ammonia: zero-carbon fertiliser, fuel and energy store. https://royalsociety.org/-/media/policy/projects/green-ammonia/green-ammonia-policy-briefing.pdf (accessed 17 September 2023).

UNCTAD, 2022. Review of Maritime Transport 2022. https://unctad.org/system/files/official-document/rmt2022_en.pdf (accessed 24 July 2024).

UNCTAD, 2023. Review of Maritime Transport 2023. https://unctad.org/system/files/official-document/rmt2023_en.pdf (accessed 17 September 2023)

Wang, H., Daoutidis, P., Zhang, Q., 2023. Ammonia-based green corridors for sustainable maritime transportation. *Digital Chemical Engineering* 6, 100082. https://doi.org/10.1016/j.dche.2022.100082

Wang, X., Jin, C., Zheng, H., Xu, S., Wu, S., Wang, C., 2023. A two-phase optimization model for low-sulphur operation of container liners in the context of carbon neutrality. *Ocean Engineering* 286, 115669. https://doi.org/10.1016/j.oceaneng.2023.115669

Wang, S., Meng, Q., 2012. Sailing speed optimization for container ships in a liner shipping network. Transportation *Research Part E-Logistics and Transportation Review* 48, 701-714. https://doi.org/10.1016/j.tre.2011.12.003

Wang, S., Meng, Q., 2017. Container liner fleet deployment: A systematic overview. *Transportation Research Part C-Emerging Technologies* 77, 389-404. https://doi.org/10.1016/j.trc.2017.02.010

Wang, S., Notteboom, T., 2015. The role of port authorities in the development of LNG bunkering facilities in North European ports. *WMU Journal of Maritime Affairs*, 14, 61-92. https://doi.org/10.1007/s13437-014-0074-9

Wang, Y., Meng, Q., Kuang, H., 2018. Jointly optimizing ship sailing speed and bunker purchase in liner shipping with distribution-free stochastic bunker prices. *Transportation Research Part C-Emerging Technologies* 89, 35-52. https://doi.org/10.1016/j.trc.2018.01.020

Wang, Y., Wang, S., 2021. Deploying, scheduling, and sequencing heterogeneous vessels in a liner container shipping route. *Transportation Research Part E-Logistics and Transportation Review* 151, 102365. https://doi.org/10.1016/j.tre.2021.102365

Waterfront Shipping, 2021. Waterfront Shipping takes leadership role in demonstrating simplicity of methanol bunkering to marine industry. https://www.waterfront-shipping.com/news/2021/05/waterfront-shipping-takes-leadership-role-demonstrating-simplicity-methanol-bunkering (accessed 25 September 2023).

Wu, Y., Huang, Y., Wang, H., Zhen, L., Shao, W., 2023. Green technology adoption and fleet deployment for new and aged ships considering maritime decarbonization. *Journal of Marine Science and Engineering* 11, 36. https://doi.org/10.3390/jmse11010036

Wu, Y., Zhang, H., Li, F., Wang, S., Zhen, L., 2023. Optimal selection of multi-fuel engines for ships considering fuel price uncertainty. *Mathematics* 11, 3621. https://doi.org/10.3390/math11173621

Wu, Y., Huang, Y., Wang, H., Zhen, L., 2022a. Joint planning of fleet deployment, ship refueling, and speed optimization for dual-fuel ships considering methane slip. *Journal of Marine Science and Engineering* 10, 1690. https://doi.org/10.3390/jmse10111690

Wu, Y., Huang, Y., Wang, H., Zhen, L., 2022b. Nonlinear programming for fleet deployment, voyage planning and speed optimization in sustainable liner shipping. *Electronic Research Archive* 31, 147-168. https://doi.org/10.3934/era.2023008

Xu, M., Deng, W., Zhu, Y., LÜ, L., 2023. Assessing and improving the structural robustness of global liner shipping system: A motif-based network science approach. *Reliability Engineering & System Safety* 240, 109576. https://doi.org/10.1016/j.ress.2023.109576

Yang, M., Lam, J.S.L., 2023. Operational and economic evaluation of ammonia bunkering – Bunkering supply chain perspective. *Transportation Research Part D: Transport and Environment* 117, 103666. https://doi.org/10.1016/j.trd.2023.103666

You, Y., Kim, S., Lee, J.C., 2023. Comparative study on ammonia and liquid hydrogen transportation costs in comparison to LNG. *International Journal of Naval Architecture and Ocean Engineering* 15, 100523. https://doi.org/10.1016/j.ijnaoe.2023.100523

Zhao, Y., Chen, Y., Fagerholt, K., Lindstad, E., Zhou, J., 2023. Pathways towards carbon reduction through technology transition in liner shipping. *Maritime Policy & Management*, 1-23. https://doi.org/10.1080/03088839.2023.2224813

Zhao, Y., Ma, Y., Peng, Z., Zhou, J., 2024. A risk-based decision-making scheme for short-sea liner fleet renewal to achieve carbon reduction targets. *Research in Transportation Business & Management* 54, 101112. https://doi.org/10.1016/j.rtbm.2024.101112

Zhao, S., Duan, J., Li, D., Yang, H., 2022. Vessel scheduling and bunker management with speed deviations for liner shipping in the presence of collaborative agreements. *Ieee Access* 10, 107669-107684. https://doi.org/10.1109/ACCESS.2022.3211311

Zhen, L., Hu, Z., Yan, R., Zhuge, D., Wang, S., 2020. Route and speed optimization for liner ships under emission control policies. *Transportation Research Part C: Emerging Technologies* 110, 330-345. https://doi.org/10.1016/j.trc.2019.11.004

Zou, J., Yang, B., 2023. Evaluation of alternative marine fuels from dual perspectives considering multiple vessel sizes. *Transportation Research Part D: Transport and Environment* 115, 103583. https://doi.org/10.1016/j.trd.2022.103583

Zou, F.-k., Zeng, H., Wang, H.-y., Wang, X.-x., Xu, Z.-x., 2021. Implementation and Parameter Analysis of the Knock Phenomenon of a Marine Dual-Fuel Engine Based on a Two-Zone Combustion Model. *Processes* 9(4), 602. https://doi.org/10.3390/pr9040602